Journal of Hazardous Materials 500 (2025) 140404

Contents lists available at ScienceDirect

Journal of Hazardous Materials

journal homepage: www.elsevier.com/locate/jhazmat

Phytochemical-driven detoxification: Impact of *Ageratina adenophora* application on heavy metal bioavailability, pathogens, and antibiotic resistance genes removal in composting systems

Yousif Abdelrahman Yousif Abdellah [a,b,*], Dou Tingting [a,c], Jianou Gao [a], Shimei Yang [a], Zhenyan Yang [a], Chengmo Yang [a], Ayodeji Bello [d,e], Elsiddig A.E. Elsheikh [f], Dong Liu [a,**], Fuqiang Yu [a,**]

[a] *Yunnan Key Laboratory for Fungal Diversity and Green Development & Yunnan International Joint Laboratory of Fungal Sustainable Utilization in South and Southeast Asia, Germplasm Bank of Wild Species, Kunming Institute of Botany, Chinese Academy of Sciences, Kunming, Yunnan Province 650201, China*
[b] *Faculty of Public and Environmental Health, University of Khartoum, Khartoum 11111, Sudan*
[c] *School of Ecology and Environmental Science, Yunnan University, Kunming 650500, China*
[d] *Southern Piedmont Agricultural Research and Extension Center, Virginia Tech, Blackstone, VA 23824, USA*
[e] *School of Plant and Environmental Sciences, Virginia Tech, Blacksburg, VA 24061, USA*
[f] *Department of Applied Biology, College of Sciences, University of Sharjah, UAE*

HIGHLIGHTS

- Higher *A. adenophora* application ratios (7.5–10 %) significantly reduced metal bioavailability.
- AA application suppressed pathogens (>90 %) via phytochemical-mediated antimicrobial activity.
- ARGs reduction in AA treatments is linked to AA-driven shifts in microbial structure.
- AA application increased TN, TP, and TK by ≥ 1.25-fold, ≥ 11-fold, and ≥ 3.60-fold, respectively.

GRAPHICAL ABSTRACT

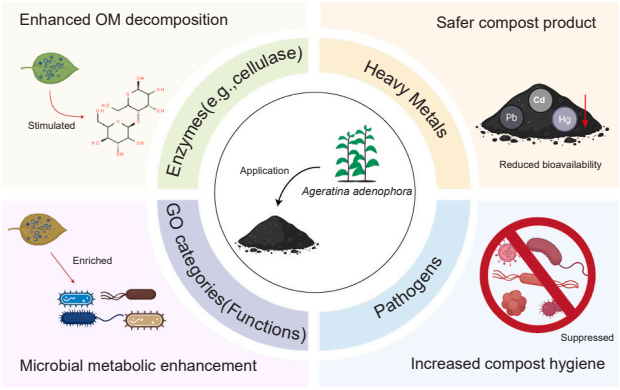

ARTICLE INFO

Keywords:
Invasive plant
Composting
Heavy metals

ABSTRACT

The invasive *Ageratina adenophora* (AA) shows promise for sustainable waste management by producing nutrient-rich organic fertilizer. However, its ability to reduce environmentally hazardous components remains unstudied. In this study, the role of AA (2.5 %–10 % w/w) in composting systems, focusing on its phytochemical-driven

* Corresponding author at: Yunnan Key Laboratory for Fungal Diversity and Green Development & Yunnan International Joint Laboratory of Fungal Sustainable Utilization in South and Southeast Asia, Germplasm Bank of Wild Species, Kunming Institute of Botany, Chinese Academy of Sciences, Kunming, Yunnan Province 650201, China.
** Corresponding authors.
E-mail addresses: yousif@mail.kib.ac.cn (Y.A.Y. Abdellah), liudongc@mail.kib.ac.cn (D. Liu), fqyu@mail.kib.ac.cn (F. Yu).

https://doi.org/10.1016/j.jhazmat.2025.140404
Received 19 June 2025; Received in revised form 16 September 2025; Accepted 5 November 2025
Available online 6 November 2025

Antibiotic degradation
Organic fertilizer

detoxification capabilities, including the bioavailability of heavy metals, pathogen suppression, and the removal of antibiotic resistance genes (ARGs), was evaluated. Results showed that AA treatments at 7.5 % and 10 % significantly decreased bioavailable Zn (80.4 %-84.4 %), Cu (94.6 %-97.8 %), Cr (59 %-73.9 %), and Pb (58.8 %-80.2 %) via humification and microbial biosorption. Pathogens (*Xanthomonas campestris*, *Staphylococcus aureus*, *Salmonella enterica*) were suppressed by ≥ 90 %, due to phytochemical-mediated antimicrobial activity. Key ARGs (*NmcR, oleC, adel*) declined by ≥ 90 % in 5 %–10 % AA treatments, while *MexS* and *mlaf* dropped by ≥ 75 % in the 10 % AA treatment, probably because of phytochemical-driven microbial community restructuring. AA also significantly enhanced nutrient retention, with total nitrogen (TN) increasing by ≥ 1.25-fold (reaching 2.15-fold in 10 % AA), total phosphorus (TP) by ≥ 11-fold (reaching 15.6-fold in 10 % AA), and total potassium (TK) by ≥ 3.60-fold (reaching 7.50-fold in 10 % AA). Simultaneously, the germination index rose to ≥ 95.3 %. Mantel tests showed strong negative correlations between phytochemicals, pathogens, and metal bioavailability, indicating an additional layer of suppression and microbial/chemical immobilization during composting. Further studies are needed to evaluate long-term ecological risks and compare AA with traditional amendments like biochar. Overall, the findings suggest AA's potential for sustainable waste management and soil remediation.

1. Introduction

The rapid acceleration of global urbanization and industrialization has precipitated a critical increase in environmental pollution, particularly from persistent and toxic contaminants such as heavy metals and antibiotics. Heavy metal pollution, stemming from industrial effluents, agricultural practices, and electronic waste, compromises soil and water quality, posing severe threats to ecological balance and human health due to their non-biodegradable nature, bioaccumulation potential, and toxicity [1,2]. Concurrently, the proliferation of antibiotic resistance, driven by the overuse and improper disposal of antibiotics in medicine and agriculture, has led to the widespread emergence and dissemination of antibiotic resistance genes (ARGs) in the environment [2–4]. These ARGs undermine the efficacy of essential antimicrobial therapies, representing one of the most pressing challenges to global public health. Developing effective strategies to co-remediate these dual threats is therefore imperative for ensuring ecosystem sustainability and safeguarding human health.

Composting has emerged as a viable and sustainable strategy for organic waste management, offering a pathway to transform waste into nutrient-rich amendments that enhance soil fertility and structure [5,6]. Beyond waste reduction and resource recovery, the composting process itself can attenuate certain pollutants through thermal inactivation, microbial degradation, and immobilization. However, the inherent efficacy of conventional composting in eliminating complex biological pollutants, particularly antibiotic residues, ARGs, and bioavailable heavy metals, is often incomplete and highly variable [6]. This limitation has spurred research into the use of complementary amendments, such as biochar, clay minerals, humic acid, and microbial inoculants, to enhance the composting process's detoxification potential [7–9].

Recently, the use of phytoremediation agents directly within composting (phytocomposting) has gained interest for its potential to leverage plant-derived compounds for pollutant mitigation [10–12]. In this context, invasive plant species represent a paradoxical resource; although they threaten biodiversity and ecosystem stability, their high biomass and often unique phytochemical profiles make them intriguing candidates for sustainable waste valorization [13,14]. *Ageratina adenophora* (AA), commonly known as Crofton weed or Mexican aster, stands out for its robust phytochemical profile, which includes flavonoids, phenolics, phthalates, and unique terpenoid compounds such as 4,7-dimethyl-1-(propan-2-ylidene)-1,4,4a,8a-tetrahydronaphthalene-2,6(1 H,7 H)-dione (DTD) and 6-hydroxy-5-isopropyl-3,8-dimethyl-4a,5,6,7,8,8a-hexahydronaphthalen-2(1 H)-one (HHO) [13–15]. These compounds exhibit documented antimicrobial, phytotoxic, and metal-chelating properties [16,17]. These compounds exhibit antibacterial, antifungal, antioxidant, and metal-chelating activities, making AA a potential dual-purpose agent for detoxification and biological risk suppression.

Compared to other invasive plants such as *Mikania micrantha*, AA offers distinct advantages: its phytochemicals are not only more diverse but also present in higher concentrations, and several of them, particularly DTD and HHO, have demonstrated potent metal binding and bactericidal properties in vitro [5,13,17,18]. AA has also been reported to influence soil microbial communities, enhance nutrient cycling, and inhibit phytopathogens, hinting at its potential as a bioactive composting amendment [16].

Preliminary evidence suggests that AA biomass can influence microbial dynamics. Studies indicate that incorporating AA in composting can modulate microbial community structure and enhance activity during the later stages of decomposition [11,13,19]. Furthermore, AA extracts demonstrate significant inhibitory effects against pathogenic bacteria such as *Pseudomonas aeruginosa* and *Bacillus cereus*, although the plant itself shows a capacity to accumulate heavy metals [11,15,17,19], supporting its application in phytoremediation strategies. This combination of properties suggests that AA could act as a multi-functional composting amendment, simultaneously suppressing pathogens, immobilizing heavy metals, and potentially mitigating ARGs by restructuring the microbial community. However, a critical knowledge gap exists. Although previous research has explored AA's antimicrobial effects in isolation or its use as a compost ingredient, no study has systematically investigated the dose-dependent efficacy and mechanistic role of its specific phytochemicals in the co-remediation of heavy metals, pathogens, and ARGs within a composting matrix. The interplay between AA's phytochemicals, the evolving microbial community, and the resultant pollutant fate remains largely unknown.

Therefore, this study aims to bridge this gap by employing a metagenomics-guided approach to evaluate the impact of AA amendment on composting efficiency and safety. We hypothesize that the addition of AA will drive a phytochemical-mediated restructuring of the microbial community, leading to the enhanced immobilization of heavy metals, suppression of pathogenic bacteria, and attenuation of ARGs. The specific objectives were to: (1) quantify the dose-dependent effects of AA (2.5–10 % w/w) on the bioavailability of Zn, Cu, Cr, and Pb; (2) assess its efficacy in reducing pathogenic bacteria and the abundance of high-risk ARGs; (3) evaluate its influence on enzyme activities, nutrient retention, and compost maturity; and (4) elucidate the underlying mechanisms by correlating phytochemical persistence with changes in the microbial community structure and functional gene profiles. By elucidating these mechanisms, this research seeks to transform an invasive ecological threat into a valuable resource for producing safe, high-quality compost, offering a novel and sustainable strategy for integrated environmental remediation.

2. Materials and methods

2.1. Composting feedstocks

The raw materials, cattle manure (CM) and spent mushroom

substrate (SMS), were collected from a nearby state-owned cattle farm and a mushroom cultivation factory (103°29′E; 26°41′N) in Kunming City, Yunnan Province, China. The biomass of *A. adenophora* (AA) was obtained from the Kunming Institute of Botany, Chinese Academy of Sciences, Yunnan, China (27°72′N, 102°25′E, 1875 m above sea level). Before mixing in the composting, the AA biomass was air-dried and mechanically chopped into pieces 2–5 cm long. The basic physico-chemical properties of CM, SMS, and AA are provided in the supplementary information (Table S1).

2.2. Composting system and protocols

The composting experiment was carried out at the Kunming Institute of Botany's Research Station in Kunming, China (25°08′56.8″N, 102°44′03.8″E), using five different treatments (Fig. 1). Composting systems were set up in custom-modified 160-L polyethylene containers (0.8 m height × 0.5 m diameter) equipped with aeration features. Ventilation holes (10 mm in diameter) were strategically positioned at the top, middle, and bottom sections of each container, with each hole placed 90 mm from the container edges to ensure optimal air distribution. The composting substrates included a mixture of SMS and CM at a weight ratio of 3.3:1. Treatments received different addition ratios (2.5 %, 5 %, 7.5 %, and 10 %; w/w) of AA residues. The control (CK) contained no additives. The initial moisture content of all mixtures was adjusted to 65 % (±2 %) for optimal microbial activity. An active aeration system was used with 10-mm diameter polyvinyl chloride pipes connected to air compressors, positioned at the top and sides of each container. Aeration was maintained at 0.025 L/min and delivered in 15-minute pulses every 8 h throughout the 56-day composting process, following established protocols from our previous research [18]. Manual turning was done weekly to promote even decomposition.

To improve the biodegradation process, all treatments were inoculated with a commercial microbial consortium [Weifang Yihao Biotechnology Co., Ltd, China; Approval No. (2791)], which includes lignocellulolytic strains *Bacillus subtilis* and *Bacillus laterosporus* at a minimum level of 5 × 10^7 CFU/g. The solid inoculum was prepared by dissolving 10 g of the product in 1 L of sterile 0.85 % saline solution, creating a stock suspension. This was then diluted 100 times with sterile deionized water to obtain the final concentration. The diluted inoculum was evenly sprayed onto the composting mixtures while turning them to ensure uniform distribution. Additionally, urea (Yunnan Yuntianhua Co., Ltd. Batch number UREA-20240518–03) was added at ratio of 1.5 % w/w to all mixtures for two main reasons: (i) to maintain an appropriate C/N ratio for microbial growth and decomposition, and (ii) to prevent N immobilization and microbial inhibition caused by the high carbon content and phytotoxic compounds (such as DTD and HHO) in AA residues [15].

2.2.1. Determination of phytochemical properties

Previous phytochemical studies identified 100 unique phytochemicals in AA [1,2], with two main compounds selected for quantitative analysis: DTD (4,7-dimethyl-1-(propan-2-ylidene)-1,4,4a,8a-tetrahydronaphthalene-2,6 (1 H,7 H)-dione) and HHO (6-hydroxy-5-isopropyl-3,8-dimethyl-4a,5,6,7,8,8a-hexahydronaphthalen-2 (1 H)-one) [13,14,20]. Their high concentrations and known antimicrobial and chelating properties made them ideal candidates for evaluating AA's detoxification efficacy [11,13,14,17]. For extraction, 50 g of compost samples from days 1, 7, 35, and 56 were homogenized in 500 mL of deionized water. The mixture was heated at 40°C with constant stirring at 120 rpm for 30 min, then centrifuged at 10,000 × g for 20 min to collect the supernatant. The levels of DTD and HHO were measured using an L-2000 series high-performance liquid chromatography system (Eclipse Plus, USA), according to Liu et al. [14]. Separation was performed on a GS-310 C18 reversed-phase column (4.6 mm × 150 mm) with an isocratic mobile phase of methanol and water (70:30 v/v) at a 1.0 mL/min flow rate under 1.5 MPa pressure. Each sample injection was 10 μL, automated for consistency.

2.2.2. Measurement of heavy metal bioavailability

Assessing heavy metal bioavailability during composting is essential

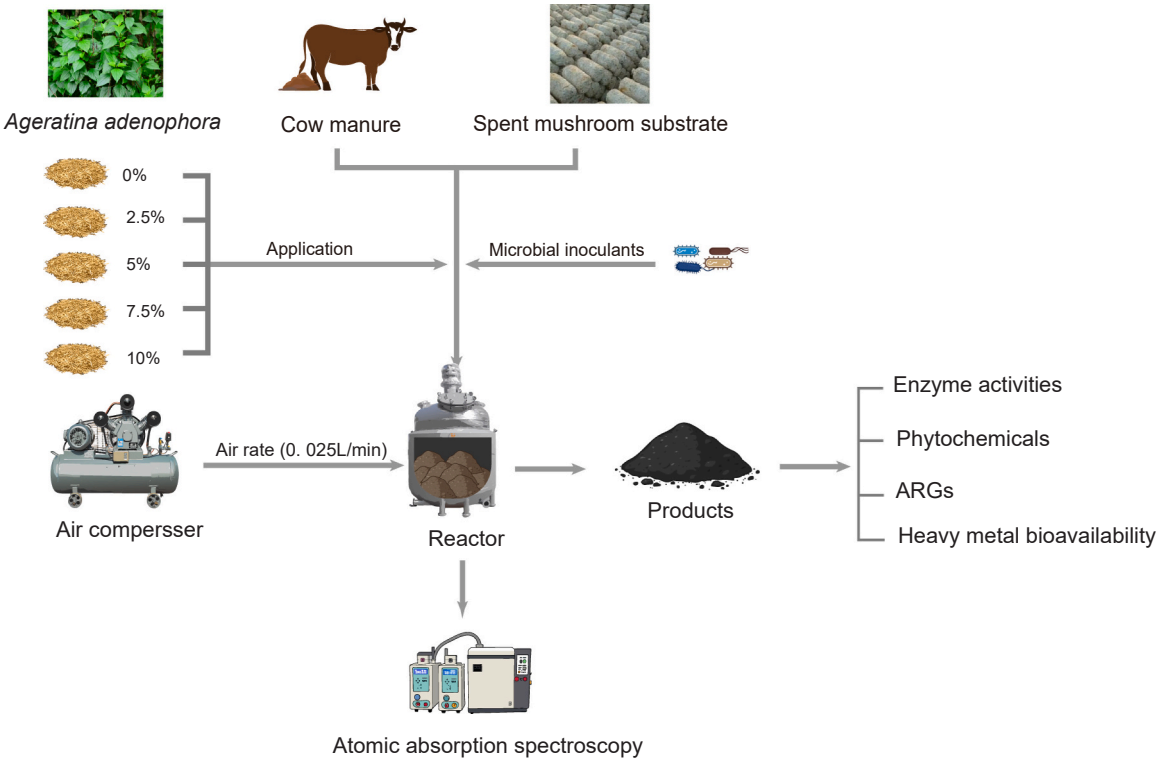

Fig. 1. Composting experimental design from raw material preparations to the final compost product quality.

for understanding environmental risks associated with using compost as a soil amendment [5,21]. In this study, heavy metal fractions were measured at Nanjing Convinced-test Technology Co., Ltd (Nanjing, China), and calculated in triplicate using the modified BCR (European Community Bureau of Reference) sequential extraction procedure [5]. Zn, Cu, Cr, and Pb were categorized as acid extractable (AcidExt) (F1), reducible (Red) (F2), oxidizable (Oxi) (F3), and residual (Res) (F4) fractions, arranged from highest to lowest bioavailability [5]. F1 and F2 are stable fractions used to estimate the mobility and bioavailability of Zn, Cu, Cr, and Pb. Meanwhile, F3 and F4 represent non-bioavailable heavy metal fractions that can be used to assess Zn, Cu, Cr, and Pb toxicity. Zn, Cu, Cr, and Pb concentrations were measured using flame atomic absorption spectrophotometry.

2.2.3. Determination of physicochemical properties

The temperature was checked daily by inserting the thermometer at three different positions (upper, middle, and bottom) of the compost, and then the average was calculated. The total organic carbon (TOC), pH, total nitrogen (TN), total potassium (TK), and total phosphorus (TP) were measured at Nanjing Convinced-test Technology Co., Ltd (Nanjing, China), according to standard methods [6].

2.2.4. Enzyme activity assessments

Five enzyme activities, cellulase, lignin peroxidase, laccase, urease, and protease, were evaluated at Nanjing Convinced-test Technology Co., Ltd (Nanjing, China). These enzymes are vital for composting, especially in breaking down lignocellulosic materials. The detailed methods are outlined in Liu et al. [22]. One enzyme activity unit equals 1.0 μg of substrate degraded per minute per 1.0 g of compost sample. In contrast, lignin peroxidase activity is defined as the production of 1.0 μmol of veratraldehyde from veratryl alcohol per minute [22].

2.2.5. Metagenomic analysis

Compost samples were collected in triplicate from treatments and CK composting groups and sent for sequencing at Shanghai Personal Biotechnology (Shanghai, China). Genome sequencing was performed on the Illumina NovaSeq 6000 platform using paired-end technology (PE 150). The raw data from the Illumina platform were filtered with FASTP (version 0.18.0) based on the following criteria: 1) removal of reads with $\geq$ 10 % unidentified nucleotides (N); 2) removal of reads where $\geq$ 50 % of bases had Phred quality scores $\leq$ 20; and 3) removal of reads aligned to barcode adapters. After filtering, the clean reads were used for genome assembly. Each sample's clean reads were assembled separately using MEGAHIT (version 1.1.2), with a k-mer range of 21–99 to generate sample-specific assemblies [23]. Gene prediction was carried out on the final assembly contigs (> 500 bp) using Metagene Mark (version 3.38). Predicted genes were clustered with CD-HIT at 95 % identity and 90 % coverage thresholds to create non-redundant gene catalogs (NRG). Representative sequences from the NRG were annotated using DIAMOND (version 0.9.24), aligning them with sequences from various protein databases, including the NCBI non-redundant protein (NR) database and eggNOG for gene orthology. Additional annotations involved databases such as Carbohydrate-Active Enzymes (CAZymes), Pathogen-Host Interactions (PHI), VFDB for virulence factors, and the Comprehensive Antibiotic Resistance Database (CARD). The abundance of antibiotic resistance genes (ARGs) and virulence factors (VFs) was calculated by assessing the abundance ratio of each gene [23]. The raw sequencing data have been deposited in the NCBI under accession No. PRJNA1241463.

2.2.6. Data visualization and statistical analyses

Statistical analysis was performed using SPSS 18.0 (IBM, USA). All data were checked for normality and variance homogeneity before analysis, using the Shapiro-Wilk test. Significant differences were identified through one-way ANOVA, with a p-value threshold of $\leq$ 0.05. Figures were created with Origin Pro (version 2022, Origin Lab, USA) and Prism GraphPad (version 8.0, San Diego, CA). The R 'vegan' package (http://cran.stat.sfu.ca/) was employed for Mantel test analysis to explore the relationships among phytochemicals, physicochemical properties, enzymes, pathogens, GO level 1, and heavy metal bioavailability.

3. Results and discussion

3.1. Phytochemical profiles during the composting process

AA-related phytochemicals (DTD and HHO) undergo rapid decomposition during composting regardless of the addition ratio (Fig. 2). In the early stages of composting, treatments with AA 2.5 %, AA 5 %, AA 7.5 %, and AA 10 % showed higher DTD levels (Fig. 2a). As the temperature increased (Fig. S1), DTD levels significantly dropped by 19 %, 13 %, 9 %, and 5.5 %, respectively, following a dose-dependent pattern on day 7 of composting. By day 35, DTD levels decreased to 89.2 %, 74 %, 71.2 %, and 65.5 %, respectively, indicating the influence of the thermophilic stage in speeding up the phytochemical degradation process [24]. On day 56, residual DTD in all treatments was 5.1 %, 9.4 %, 14.6 %, and 18.1 %, respectively, demonstrating the effectiveness of the composting process in managing phytochemical levels. Conversely, higher AA application rates (AA 7.5 % and AA 10 %) resulted in slower DTD degradation, pointing to potential inhibitory effects at elevated application levels.

HHO showed the same pattern as DTD, but with lower initial levels during the early stage of composting (Fig. 2b). These levels decreased by 74.3 %, 80.2 %, 87 %, and 93.1 % on day 7, and by 4.6 %, 8 %, 10.5 %, and 13.8 % on day 56 in the AA 2.5 %, AA 5 %, AA 7.5 %, and AA 10 % treatments, respectively. This steady reduction suggests that microbes in the composting system actively break down these phytochemicals over time. For instance, in similar studies on composting AA-derived compounds, examining the degradation of phenolic compounds during composting agricultural residues, the levels of target compounds decreased due to bacterial and fungal activity [11,13,14]. Lower AA application rates (AA 2.5 % and 5 %) are more effective at degrading DTD, likely because of balanced microbial activity. Conversely, higher AA application rates (7.5 % and 10 %) may slow degradation somewhat due to initial phytochemical toxicity. This indicates that the degradation of DTD and HHO is concentration-dependent, with higher AA phytochemical concentrations leading to gradual breakdown. Ultimately, the degradation of DTD and HHO can also influence the quality of the resulting organic fertilizer, as the breakdown products could potentially contribute to humic substance formation or supply plant nutrients [15].

3.2. Pollutant mitigation efficiency during composting in response to AA application rates

3.2.1. Heavy metal bioavailability variations

To elucidate the specific mechanisms behind the reduced metal bioavailability, a sequential extraction analysis was performed to quantify the distribution of Zn, Cu, Cr, and Pb into four operationally defined fractions: exchangeable (F1), carbonate-bound (F2), organic matter-bound (F3), and residual (Fig. 3 and Table S2). On the initial composting day, the AA treatments and CK start with relatively high bioavailable Zn levels, exhibiting no significant differences ($p \geq 0.05$) (Fig. 3). Meanwhile, on day 7, a noticeable decrease in bioavailable Zn is observed in all groups compared to day 1, with the CK and AA 2.5 % treatment disclosing slightly higher levels than the other AA treatments (Fig. 3a). This suggests that adding higher AA rates besides the impact of microbial immobilization during active decomposition of composting [25] might influence the bioavailability of Zn during composting. Significant declines in bioavailable Zn are evident in all AA treatments, particularly in the AA 7.5 % and AA 10 % treatments at day 35 ($p < 0.05$). By day 56, the bioavailable Zn levels in the AA 10 % treatment are the lowest among all groups (Fig. 3 and Table S2), suggesting

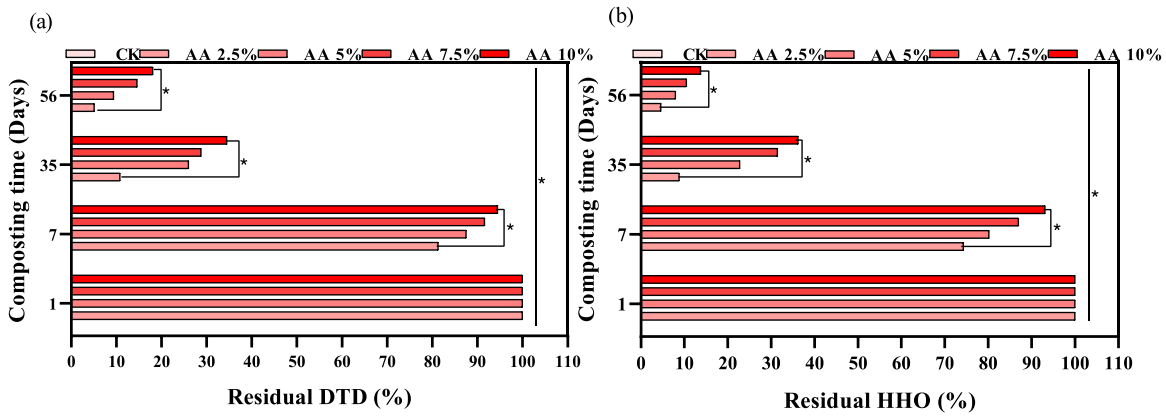

Fig. 2. Phytochemical profiles and dynamics; (a) DTD dynamics; and (b) HHO dynamics during the composting process under different treatments: CK (control), AA 2.5 %, AA 5 %, AA 7.5 %, and AA 10 %. AA represents the treatment with the addition ratio of *A. adenophora*: AA 2.5 %, AA 5 %, AA 7.5 %, and AA 10 %. CK represents the control treatment of cattle manure and spent mushroom substrate. Results are the mean of three replicates, and error bars indicate standard deviation (SD). Significant differences in phytochemicals across the AA treatments and CK are represented by * $p < 0.05$.

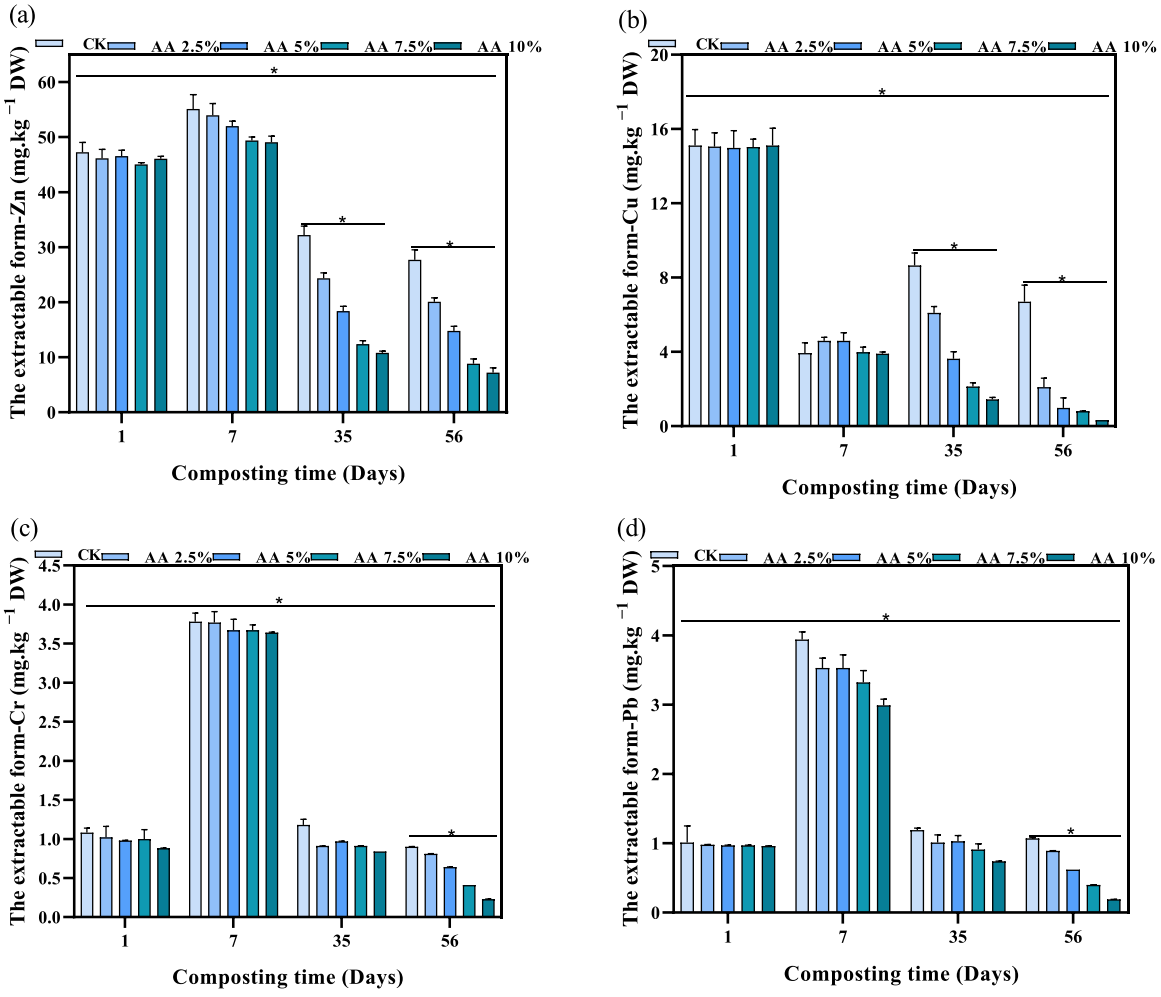

Fig. 3. The changes in heavy metal bioavailability; bioavailable Zn (a), bioavailable Cu (b), bioavailable Cr (c), and bioavailable Pb (d) during the composting process under different treatments: CK (control), AA 2.5 %, AA 5 %, AA 7.5 %, and AA 10 %. AA represents *A. adenophora* additive. AA represents the treatment with the application ratio of *A. adenophora*: AA 2.5 %, AA 5 %, AA 7.5 %, and AA 10 %. CK represents the control treatment of cattle manure and spent mushroom substrate. Results are the mean of three replicates, and error bars indicate standard deviation (SD). Significant differences in heavy metal bioavailability across the AA treatments and CK are represented by * $p < 0.05$.

that higher AA rates might enhance the immobilization or stabilization of Zn in the compost, which could be due to enriched organic matter and the humification process [24]. The CK group exhibits a moderate decrease in bioavailable Zn over time, although this is not as pronounced as in some AA treatments, particularly on day 56. Finally, the bioavailable Zn levels in all the treatments were as follows: AA 10 %

treatment (7.21 mg/kg) < AA 7.5 % treatment (8.81 mg/kg) < AA 5 % treatment (14.8 mg/kg) < 2.5 % treatment (20.1 mg/kg) < CK (27.7 mg/kg). Higher AA rates (7.5 % and 10 % treatments) resulted in > 80 % reduction in heavy metal bioavailability, significantly outperforming the CK (41.4 %). The AA 10 % treatment showed the highest bioavailable Zn reduction (84.3 %), demonstrating its efficacy in metal immobilization via humification and microbial activity (Table S3). This confirms AA's role in mitigating heavy metal pollution during composting, with 7.5 % and 10 % being the optimal rates.

On day 1 of composting, the CK and treatments begin with similar levels of bioavailable Cu, demonstrating comparable Cu bioavailability in the initial compost mixtures (Fig. 3b). A decrease in bioavailable Cu is observed across all treatments on day 7 compared with day 1 of composting. The AA 2.5 % and AA 5 % treatments display insignificantly higher Cu levels than CK and other AA treatments, suggesting that moderate amounts of AA may slightly enhance Cu bioavailability [21]. On day 35, significant reductions in bioavailable Cu were observed in the AA 2.5 % and AA 5 % treatments relative to CK, indicating effective Cu immobilization by AA ($p < 0.05$). The lowest bioavailable Cu levels were noted in the AA 7.5 % (2.14 mg/kg) and AA 10 % (1.44 mg/kg) treatments versus CK (8.65 mg/kg), which was strongly correlated with the accumulation of humic substances and increased microbial activity proportional to AA dosage (Mantel test, Fig. 10). This suggests AA amendment is associated with a reduction in bioavailable Zn via microbial/chemical immobilization, mitigating environmental risks [1, 3]. This suggests AA reduces bioavailable Zn via microbial/chemical immobilization, mitigating environmental risks. The bioavailable Cu levels further decreased on day 56 of composting, with the AA 10 % treatment displaying the lowest levels (0.32 mg/kg) among all AA treatments compared with CK (6.70 mg/kg). This trend suggests that higher AA rates may facilitate the precipitation or adsorption of Cu, thereby reducing its bioavailability. This could be beneficial for lowering Cu toxicity in soil when the compost is applied. Finally, all AA treatments demonstrated > 85 % Cu reduction, far exceeding CK (55.7 %). Higher AA application rates yielded greater reductions, with AA 10 % treatment achieving near-total removal (97.9 %) (Table S4). The findings demonstrate that AA application, particularly at ≥ 5 % ratios, can effectively immobilize Cu during composting through possible mechanisms of organic complexation and microbial biosorption [26].

Initial bioavailable Cr levels on day 1 of composting are relatively consistent (0.880 mg/kg to 1.08 mg/kg) across all treatments, indicating similar starting conditions (Fig. 3c). Unlike other heavy metals, on day 7 of composting, there was a significant increase in bioavailable Cr in the CK and AA treatments, compared with day 1, with the AA 10 % treatment showing the lowest level (3.64 mg/kg). This suggests that certain microorganisms can solubilize Cr, converting it into more bioavailable forms during the early stages of composting [27]. Additionally, the elevated temperatures during the thermophilic stage can alter the chemical forms of Cr present in the compost, potentially increasing its solubility and bioavailability [28]. Cr reduction gradually increased with higher AA application ratios, from 16.7 % (CK) to 73.9 % (AA 10 % treatment). The AA 7.5 % and 10 % treatments demonstrated substantially greater reductions (>59 %) compared to lower ratios (Table S5). The findings exhibit that Cr exhibits more resistant behavior than other heavy metals, but higher AA application ratios (>7.5 %) can effectively enhance its immobilization, probably via mechanisms of microbial reduction and organic complexation [26].

On day 1 of composting, all AA treatments and the CK showed similar levels of bioavailable Pb, indicating consistent initial conditions (Fig. 3d). A notable increase in bioavailable Pb was observed across all groups compared to day 1, with the CK reaching 3.94 mg/kg. The rise in temperatures and pH fluctuations during this phase likely caused changes in Pb speciation, increasing its solubility and microbial access, thereby boosting bioavailability [1]. By days 35 and 56, bioavailable Pb decreased in the AA treatments (from 0.400 mg/kg to 0.890 mg/kg), with the AA 10 % treatment showing a significant drop at day 56 (0.190 mg/kg) compared to CK (1.07 mg/kg). Higher AA application rates (AA 5 % and AA 10 %) resulted in greater reductions, with AA 10 % achieving an 80.2 % decrease in Pb (Table S6). Elevated AA ratios may promote Pb immobilization or stabilization over time through increased organic matter and humification [29]. These results align with those of Song et al. [30], who noted that certain organic additives influence the bioavailability of heavy metals in composting, as some organic materials enhance immobilization and reduce bioavailability [21].

In the end, applying AA significantly reduced the bioavailability of heavy metals like Pb, Cd, and Zn compared to CK. This reduction mainly stems from AA's phytochemical properties, such as DTD and HHO, which are capable of chelating metals and immobilizing them within the compost matrix [23]. Metal speciation analysis revealed that most metals existed in exchangeable and carbonate-bound forms, making them more susceptible to microbial biosorption and humification [3, 29]. This supports earlier research demonstrating how phytochemicals promote metal stabilization in compost systems [19,31].

3.2.2. *Pathogenic species, antibiotics, and their related gene variations during composting in response to AA application rates*

By exploring the Pathogen-Host Interactions (PHI) database, the composting process was evaluated for shifts in pathogenic microbial communities across treatments with different AA application rates (2.5 %, 5 %, 7.5 %, and 10 %) and over three composting stages (day 1, day 7, and day 56) (Fig. 4a). To examine changes in several key pathogenic taxa, such as *Pseudomonas aeruginosa, Staphylococcus aureus, Salmonella enterica,* and *Mycobacterium tuberculosis*, the responses to both AA application level and composting time were found to be dynamic. For example, the abundance of *Pseudomonas aeruginosa* decreased significantly as composting advanced from the initial to the final stages. In CK1 and CK7, the same species' abundance ranged from 0.074 to 0.034, then increased again by day 56–0.043. Meanwhile, on day 56 in the AA 7.5 % treatment, levels dropped to 0.014, and further decreased with the AA 10 % treatment to 0.010, suggesting that higher AA rates may have more effectively suppressed *P. aeruginosa* [19]. *Salmonella enterica* abundance was notably high on day 1 in CK (0.076) and declined across treatments and time points. By day 56, in the AA 10 % treatment, it was reduced to just 0.003, supporting the idea that AA may aid pathogen suppression, possibly through secondary metabolites with antimicrobial activity [16,17]. The highest abundance of *Staphylococcus aureus* (0.056) was observed on day 1 in CK, declining to 0.026 by day 56. In contrast, levels in AA treatments showed a significant decrease by day 56, especially under high AA rates (to 0.004 in AA 7.5 % and 0.002 in AA 10 %), indicating dose-dependent inhibition. It is essential to recognize that pathogen suppression in composting is a complex process involving thermal inactivation, microbial antagonism, and pH adjustments [31]. The strong negative correlations between phytochemical concentrations and pathogen abundance (Fig. 10) imply that AA-derived compounds likely add an extra layer of suppression, especially during the maturation phase as temperatures drop. Although *Mycobacterium tuberculosis* is present in lower overall amounts, the trend showed a moderate decrease over time (from 0.029 on day 1 in AA 2.5 % to 0.019 on day 56 in AA 10 %), again indicating possible antimicrobial effects associated with AA [17]. Lastly, *X. campestris, S. aureus,* and *S. enterica* showed over 90 % reduction in the AA treatments (from AA 5 % to AA 10 %). Meanwhile, *Erwinia amylovora* and *X. oryzae* achieved over 88 % reduction with AA 10 % treatment (Table S7), highlighting the role of the additive in pathogen suppression.

Aspergillus fumigatus and Fusarium graminearum, both linked to opportunistic infections, exhibited different trends. Notably, *A. fumigatus* demonstrated resilience in some treatments (such as 0.024 on day 1 in the AA 10 % treatment), although a significant decrease was observed by day 56 (0.007) in AA 10 % treatment. This indicates that fungal pathogens may be more persistent but are still impacted by

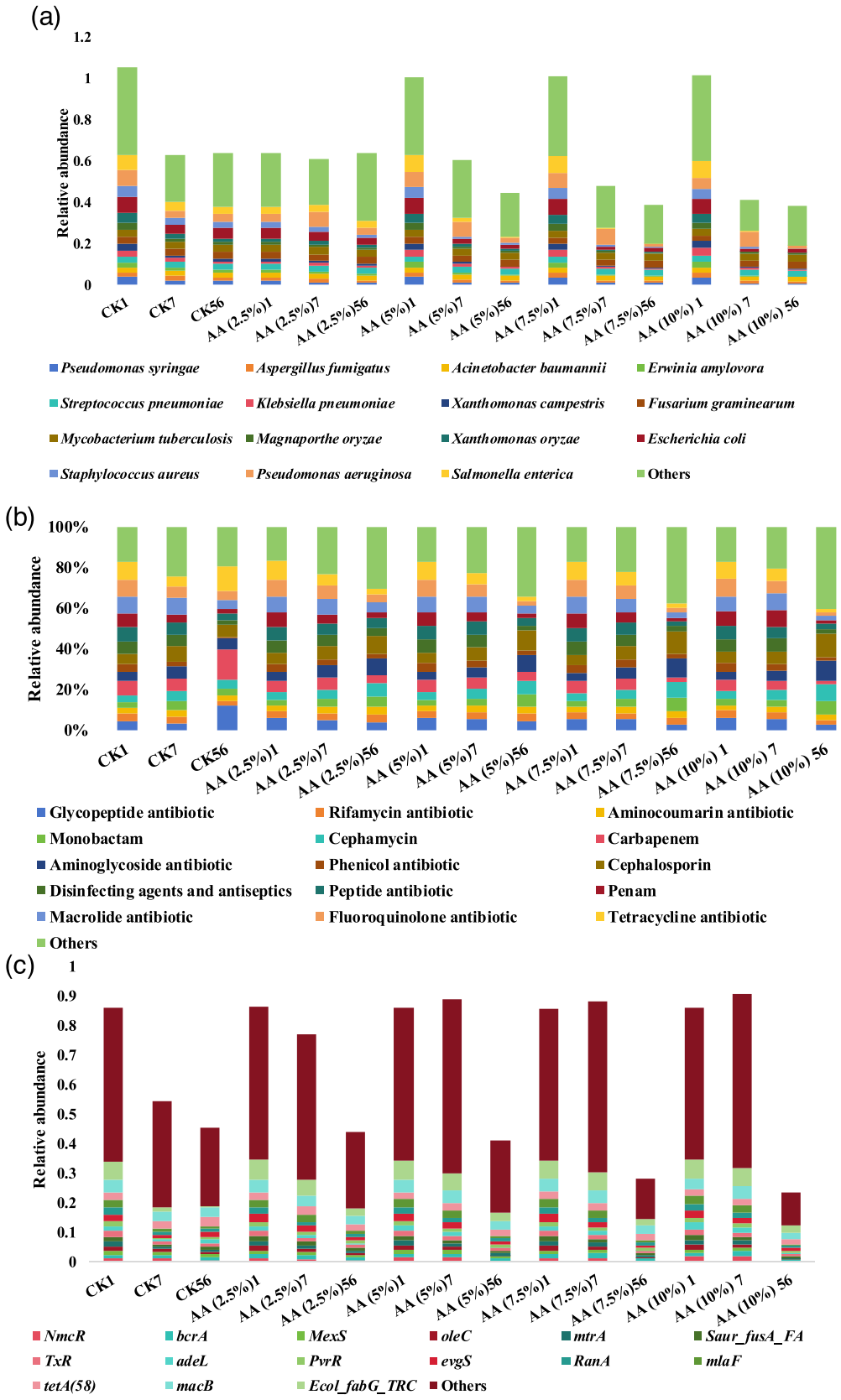

Fig. 4. The changes in pathogenic species, antibiotics and their related gene variations; top pathogenic species according to PHI (a), top abundant antibiotics according to CARD (b), and top abundant ARGs (c) during the composting process under different treatments: CK (control), AA 2.5 %, AA 5 %, AA 7.5 %, and AA 10 %. AA represents *A. adenophora* additive. AA represents the treatment with the application ratio of *A. adenophora*: AA 2.5 %, AA 5 %, AA 7.5 %, and AA 10 %. CK

represents the control treatment of cattle manure and spent mushroom substrate. Results are the mean of three replicates, and error bars indicate standard deviation (SD).

extended composting and AA exposure [17].

Through investigating the Comprehensive Antibiotic Resistance Database (CARD), the compost treated with AA showed notable shifts in antibiotic resistance-related functional categories, especially those linked to high-abundance antibiotic classes (Fig. 4b). The 15 most abundant ARG-associated terms, including resistance to glycopeptides, rifamycin, aminoglycosides, macrolides, fluoroquinolones, tetracyclines, and β-lactam classes, were monitored over time. In CK1, CK7, and CK56, terms related to tetracycline, fluoroquinolone, macrolide, and peptide antibiotic resistance were among the most prominent. For example, the abundance of tetracycline resistance in CK1 was 0.098, slightly decreasing in CK7 (0.033), and marginally lower in CK56 (0.031). Under AA treatments, the abundance of tetracycline resistance genes steadily declined with composting, from 0.099 on day 1 in AA 2.5 % treatment to 0.046 on day 7 in AA 5 % treatment, and to 0.007 on day 56 in AA 10 % treatment. This significant decrease, especially in the 10 % AA treatment, suggests that AA may facilitate the degradation or suppression of tetracycline resistance determinants [19].

The abundance of macrolide antibiotic resistance was 0.089 on day 1 of composting, then decreased to 0.061 by day 7, and further declined to 0.049. Similarly, the abundance of macrolide resistance genes decreased from 0.085 on day 1 in the AA 2.5 % treatment to 0.031 on day 7 in the AA 5 % treatment and to 0.017 on day 56 in the AA 10 % treatment. This downward trend was consistent across all treatments, indicating that composting combined with AA promotes a reduction in macrolide ARGs [3]. Fluoroquinolone antibiotic resistance abundance was 0.089 on day 1 in CK; it remained moderately high on day 7 (0.092), then decreased to 0.072 on day 56. Meanwhile, fluoroquinolone resistance genes dropped from 0.092 on day 2 in the AA 5 % treatment to 0.012 on day 56 in the AA 10 % treatment, highlighting a significant suppression effect over time and with increasing AA ratios. Glycopeptide resistance was initially moderately abundant (such as 0.106 in CK; 0.062 in the AA 5 % treatment) but declined significantly over time. By day 56, the AA 10 % treatment showed a glycopeptide resistance gene abundance of 0.0105, indicating that AA reduces the prevalence of glycopeptide resistance genes [4]. Peptide antibiotic resistance, which was 0.074 in CK on day 1, decreased gradually in the AA treatments, reaching 0.008 in the AA 10 % treatment by day 56. Rifamycin resistance dropped from 0.046 in CK1–0.0184 in the AA 2.5 % treatment and further to 0.011 in the AA 10 % treatment on day 56. Although natural composting alone (as observed in CK1 to CK56) results in some reduction in antibiotic resistance gene abundance, AA application accelerates and enhances ARG suppression, especially at 7.5 % and 10 % application rates.

The composting process resulted in a gradual decrease in the relative abundance of most ARGs over time, and this reduction was notably enhanced by increasing concentrations of AA, especially at the AA 10 % treatment. By day 56, most high-abundance ARGs were significantly lower in AA treatments compared to CK56 (Fig. 4c). For example, *tetA* (58), one of the consistently high-abundance ARGs, declined from 0.026 (CK1) to 0.021 (CK56), but was reduced even more substantially on day 56 in the AA treatments, dropping to 0.013 in AA 10 % treatment, indicating stronger attenuation at higher AA levels. *macB* (an efflux pump associated with macrolide resistance) started at 0.042 in CK1 and remained relatively high in CK56 (0.038). However, on day 56 in the AA 10 % treatment, *macB* decreased to 0.019, nearly a 50 % reduction compared to CK. *MexS*, involved in multidrug efflux resistance, followed a similar pattern, decreasing from 0.013 in CK1–0.009 in CK56. Furthermore, on day 56, the AA 10 % treatment reduced this further to 0.002, emphasizing the suppressive effect of AA on multidrug resistance genes. *evgS*, a two-component regulator associated with multiple resistance pathways, remained high in CK1 (0.025) but dropped significantly by day 56 in the AA 10 % treatment (0.012). *mtrA*, linked with efflux pump systems and known for regulating resistance in *Neisseria* and *Mycobacterium* spp., declined from 0.016 in CK1–0.0105 in CK56, and further decreased to 0.0043 on day 56 in AA 10 % treatment.

Specific ARGs exhibited rapid suppression even at early composting stages under a high AA ratio, in response to variation in ARG mechanisms (Fig.S1). For example, *Ecol_fabG_TRC*, involved in trimethoprim resistance, dropped from 0.063 in CK1–0.061 in the AA 10 % treatment on day 1 and further declined on day 56–0.023 in the AA 10 % treatment, although CK56 still retained 0.033. *adeL* and *PuvR*, transcriptional regulators of efflux pumps, demonstrated sharp declines in abundance under AA treatment, suggesting a potential inhibition of regulatory pathways for resistance. Across nearly all ARGs, the trend showed that higher ratios of AA (7.5 % and 10 % treatments) consistently resulted in the lowest ARG abundances by day 56. This suggests a dose-dependent antimicrobial or resistance-suppressive mechanism linked to phytochemicals in AA. Finally, *NmcR, oleC,* and *adel* showed $>$ 90 % reduction with the AA 5 % to AA 10 % treatments. The decrease of *NmcR, oleC,* and *adel* was closely linked to shifts in the microbial community structure. Specifically, an increase in the relative abundance of functional microbes such as *Bacillus* species and Rhodanobacteraceae was observed, known for their roles in lignin degradation and ARG reduction [3,19]. The application of AA phytochemicals likely facilitated these microbial shifts, as they promote the growth of specific microbial taxa capable of ARG degradation [32]. The abundance of *exS* and *mlaf* reached $>$ 75 % reduction in the AA 10 % treatments. Although *bcrA* and *tetA* (58) displayed increased abundance in CK, their abundances were considerably reduced [up to 54.8 % for *bcrA* and 30.3 % for *tetA* (58)] in the AA treatments (Table S8). Higher AA application rates (AA 7.5 % and AA 10 % treatments) achieved greater ARG reductions, suggesting the role of AA in accelerating degradation or suppression of ARGs [4,19].

3.3. Enzyme activity changes in response to AA application rates in the composting

On day 1 of composting, cellulase activity is relatively low across AA treatments and CK, indicating the initial phase of composting where microbial activity is just starting to proliferate (Fig. 5a). Compared with CK (4.32 mg/g/24 h) and other AA treatments (6.08 mg/g/24 h to 8.52 mg/g/24 h), a significant increase in cellulase activity is observed in the AA 10 % treatment (8.79 mg/g/24 h), implying that rapid decomposition of labile cellulose in response to addition of AA which enhances cellulase production during this stage of composting. The AA treatments and CK illustrated the highest cellulase activity at day 7, followed by a decline. The AA 7.5 % and AA 10 % treatments present the highest cellulase activity (6.14 mg/g/24 h to 6.92 mg/g/24 h), demonstrating that these supplement rates might be optimal for stimulating microbial activity and cellulose decomposition during composting. The elevated activity of cellulase in the thermophilic phase indicates accelerated breakdown of the cellulose-rich AA biomass and spent mushroom substrate. This hydrolysis is a prerequisite for releasing soluble organic compounds that serve as both a microbial energy source and a substrate for the humification process [22,33]. On day 56 of composting, the AA treatments and CK displayed a significant decline in cellulase activity ($\leq$4.0 mg/g/24 h), which might imply that the easily degradable organic matter has been consumed, leading to a decrease in available substrates for cellulase enzymes to act upon [6]. Ultimately, throughout composting, CK showed minimal change (1.2-fold), where the AA 7.5 % and AA 10 % treatments had the highest cumulative increases (5.8-fold).

Through the initial composting stage (days 1–7), both AA treatments and CK showed low lignin peroxidase activity (3.02 μg/g/h–6.1 μg/g/h) (Fig. 5b), reflecting the microbial community adaptation phase and a

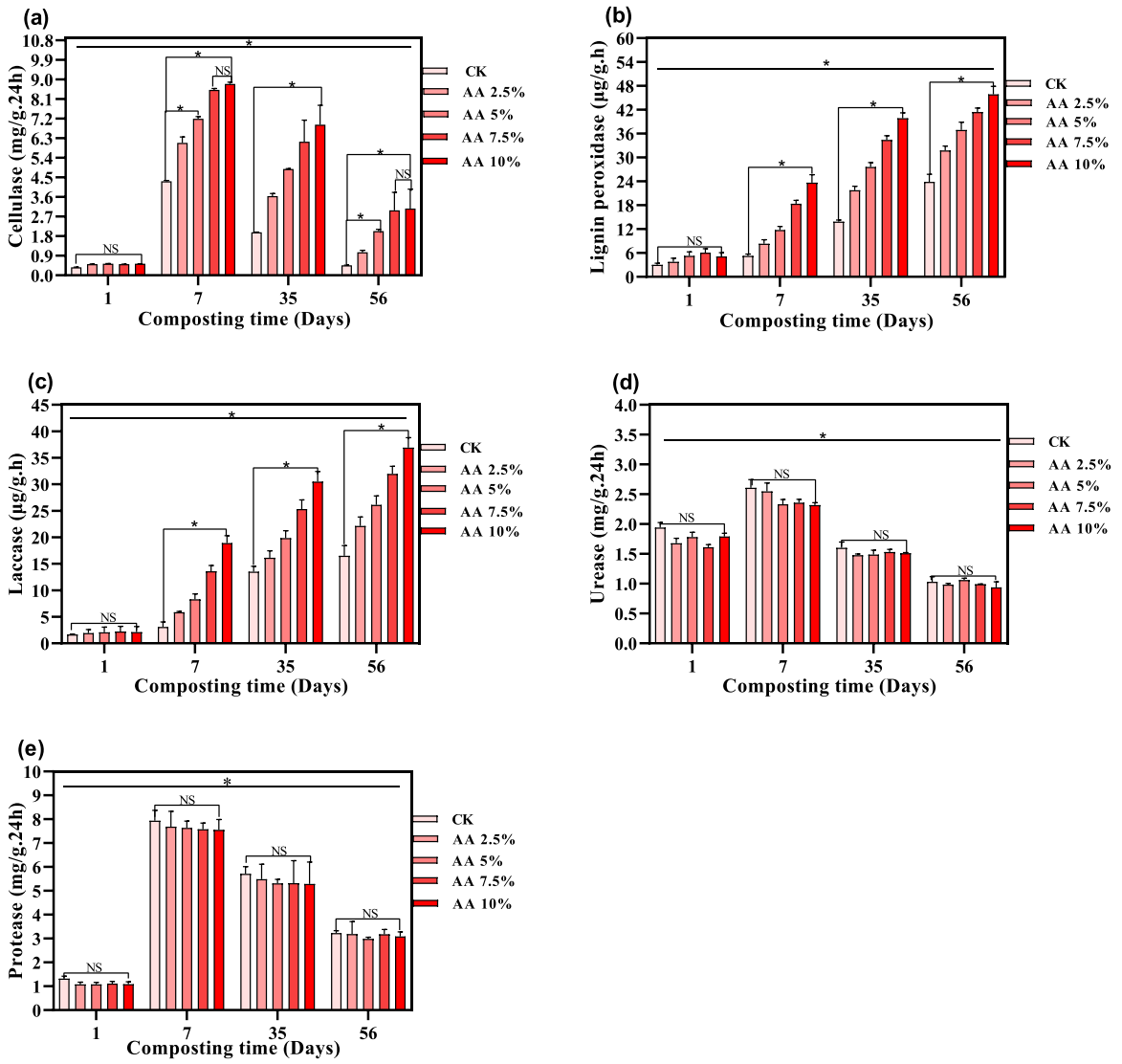

Fig. 5. Variations in enzyme activity during composting; Cellulase (a), Lignin peroxidase (b), Laccase (c), Urease (d), and Protease (e) during the composting process under different treatments: CK (control), AA 2.5 %, AA 5 %, AA 7.5 %, and AA 10 %. AA represents the treatment with the application ratio of *A. adenophora*: AA 2.5 %, AA 5 %, AA 7.5 %, and AA 10 %. CK represents the control treatment of cattle manure and spent mushroom substrate. Results are the mean of three replicates, and error bars indicate standard deviation (SD). Significant differences in enzyme activities across the AA treatments and CK are represented by * $p < 0.05$.

preference for labile carbon sources over lignin [34]. Conversely, during the maturation phase (days 35–56), AA treatments demonstrated increased lignin peroxidase activity, with AA 7.5 % and AA 10 % outperforming the CK. This suggests that higher AA concentrations may be needed to maintain high lignin peroxidase activity and facilitate lignin breakdown [32]. Ultimately, lignin peroxidase activity was highest in the order: AA 10 % (45.9 μg/g/h) > AA 7.5 % (41.4 μg/g/h) > AA 5 % (36.9 μg/g/h) > AA 2.5 % (31.8 μg/g/h) > CK (23.9 μg/g/h). The AA 10 % treatment achieved an 8.9-fold increase, indicating it as the most effective concentration for lignin degradation.

During the initial stage (day 1), both AA treatments and CK showed low laccase activity (1.66–2.23 μg/g/h) (Fig. 5c), indicating early composting with minimal microbial activity. By day 7, laccase activity rose markedly in the AA treatments (5.86–18.9 μg/g/h) compared to CK (3.08 μg/g/h), implying that AA application enhances laccase production, which is essential for lignin breakdown [34]. The activity in the AA treatments continued to improve compared to CK (16.5 μg/g/h), with the AA 10 % treatment reaching the peak at day 56 (36.9 μg/g/h). This indicates that higher AA rates (AA 5 %–AA 10 %) can more effectively stimulate laccase activity (12.5–17.5 times higher) over time. The increased laccase activity in the AA treatments is due to AA's native phenolic compounds acting as enzyme mediators [35]. The most significant response was observed in the lignin-modifying enzymes, lignin peroxidase and laccase, which exhibited a pronounced, dose-dependent increase in activity with higher AA application rates (Fig. 5b, c). This enhancement is critically linked to heavy metal immobilization. Lignin-modifying enzymes are core catalysts in the humification process, polymerizing simple phenolic compounds into complex, stable humic substances. These humic substances possess abundant functional groups (such as carboxyl, phenolic-OH) that effectively chelate and immobilize heavy metal ions, thereby reducing their bioavailability [36]. The strong negative correlations between lignin peroxidase and laccase activities and the bioavailability of Zn, Cu, and Pb (Mantel test, Fig. 10) directly support this mechanism. The higher AA treatments (7.5 % and 10 %) provided a rich source of phenolic precursors (from the breakdown of AA biomass), which likely stimulated microbial production of lignin-modifying enzymes and subsequently drove the formation of metal-stabilizing humic complexes [24,37,38].

Urease activity is relatively low across the AA treatments and CK during the initial stage (day 1), disclosing the early phase of composting

where microbial activity is minimal (Fig. 5d). Meanwhile, compared with day 1, a significant increase in urease activity is observed in the AA treatments (2.32 mg/g/24h–2.55 mg/g/24 h) in day 7, implying that this AA rate might enhance urease production during the early stages of composting. Meanwhile, CK exhibited a urease activity of 2.61 mg/g.24 h, possibly due to rapid urea hydrolysis from the composting mixture and intensive proteolysis by mesophilic microbes [39]. From day 35 to day 56 of composting, urease activity decreased (40–47 % reduction) in the AA treatments, with no significant differences observed among them, indicating completed N mineralization and ammonia volatilization equilibrium. Although CK showed the highest reduction (47 %), the AA 7.5 % treatment had the smallest reduction (38 %), suggesting slightly better retention of urease activity.

On day 1 of composting, protease activity is relatively low across the AA treatments and CK, indicating the initial stage where microbial activity is minimal (Fig. 5e). Meanwhile, on day 7 of composting, a significant increase in protease activity is observed in the AA treatments (7.55 mg/g/24h–7.69 mg/g/24 h) and even higher in CK (7.94 mg/g/24 h), contributing to the degradation of organic matter during this stage. From day 35 to day 56 of composting, protease activity decreases in the AA treatments, with no significant differences observed. However, compared with day 1, the AA treatments and CK showed substantial increases in protease activity by day 56 (2.45-fold to 2.95-fold). In addition, the AA 2.5 % treatment had the highest fold increase (2.95-fold), suggesting optimal protease enhancement at this dosage. Nonetheless, previous studies reported that protease activity generally decreases towards the end of the composting process as readily available proteins and peptides are consumed [40,41]. The sustained activity of protease and urease throughout the active composting phase points to robust N mineralization. This process releases ammonium ions, which can contribute to the precipitation of heavy metals as stable metal-ammine complexes or influence pH to favor immobilization [1,5].

Finally, the synergistic enhancement of key enzymes underpins the mechanism for detoxifying heavy metals and organic pollutants concurrently. Changes in enzyme activities, especially urease, dehydrogenase, and phosphatase, showed a complex link with how pollutants are removed. In treatments with AA, higher urease and dehydrogenase activities are associated with increased organic matter breakdown and microbial activity, both vital for humification and metal immobilization [5]. For instance, dehydrogenase activity peaked at day 14 in the 10 % AA treatment, coinciding with significant drops in bioavailable Cu and Zn, indicating active microbial biosorption and transformation. Likewise, the rise in phosphatase activity mirrored the sharp decline in ARGs like *NmcR* and *adel*, suggesting that microbial functional shifts, likely stimulated by AA phytochemicals [3], disrupted gene transfer and reduced antibiotic resistance. The Mantel test supported these findings, showing strong negative correlations between enzyme activities and both heavy metal bioavailability and pathogen levels. Overall, enzyme activity changes aligned with specific pollutant degradation phases, implying that the AA amendments help modulate compost microbiomes to enhance detoxification processes.

3.4. Nutrient level variations in response to AA application rates in the composting

From day 1 of composting, the germination index (GI) is relatively low across the AA treatments and CK, indicating that composting at this early stage may not be highly conducive to plant germination (Fig. 6a). By day 7, CK exhibited the highest GI of 40.1 % compared to the AA treatments (27.3–37.5 %). These results could be due to the high presence of phytochemicals (DTD/HHO) in the composting mixtures, which inhibit seed germination [14]. The GI in all AA treatments gradually increased as phytochemicals decreased and humic substances formed [13–15]. Compared to CK, these treatments showed higher GI on days 35 and 56 of composting, with the AA 10 % treatment reaching the highest GI rate (98.9 %), indicating more nutrients and fewer phytotoxic

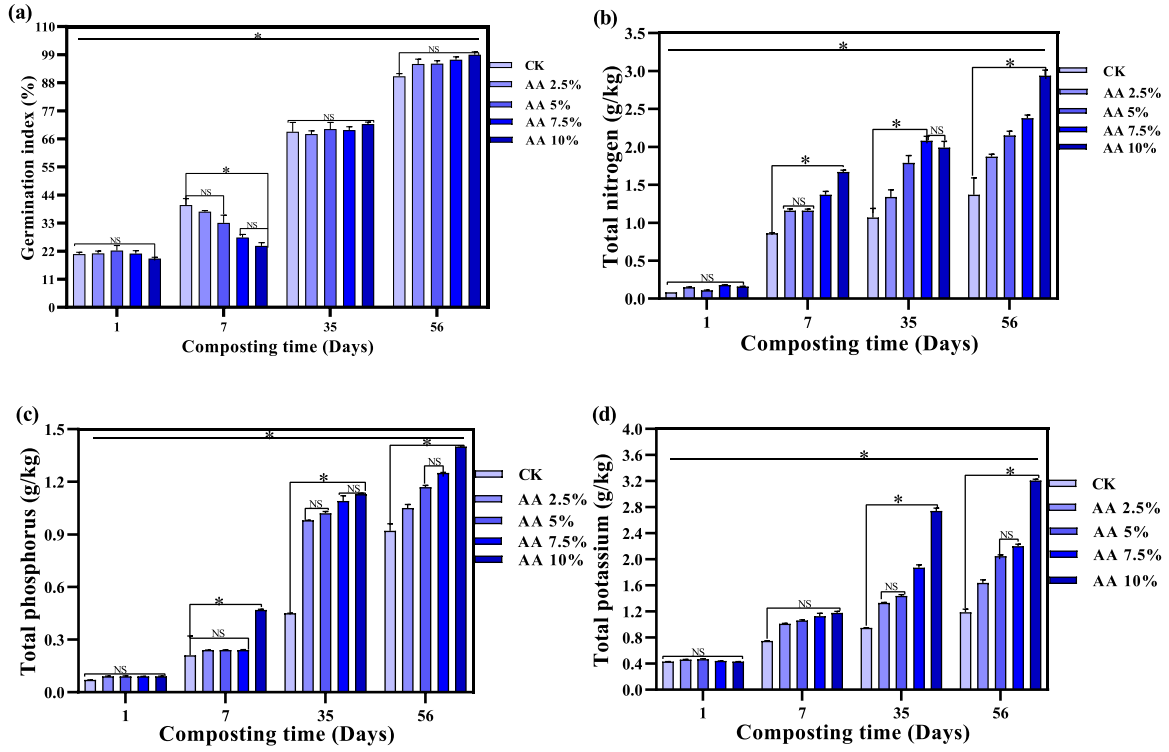

Fig. 6. The changes in nutrient levels, germination index (a), total nitrogen (b), total phosphorus (c), and total potassium (d) during the composting process under different treatments: CK (control), AA 2.5 %, AA 5 %, AA 7.5 %, and AA 10 %. AA represents the treatment with the addition ratio of *A. adenophora*: AA 2.5 %, AA 5 %, AA 7.5 %, and AA 10 %. CK represents the control treatment of cattle manure and spent mushroom substrate. Results are the mean of three replicates, and error bars indicate standard deviation (SD). Significant differences in nutrient levels across all composting groups are represented by * $p < 0.05$.

substances. At the end of composting, the final GI values ranked as follows: AA 10 % (98.9 %) > AA 7.5 % (97.1 %) > AA 5 % (95.5 %) > AA 2.5 % (95.3 %) > CK (90.6 %). The application of AA had a significant effect on the germination index during composting, especially at the final stage, with higher AA application rates (7.5 % and 10 %) resulting in higher indices. This suggests that AA application can boost nutrient and humic substance levels while reducing phytotoxic compounds such as phytochemicals, volatile fatty acids, and ammonium [18].

The AA treatments and CK illustrated a gradual increase in TN during the early composting stage (1–7 days) (Fig. 6b), probably due to organic matter mineralization and microbial activity [42]. From day 35–56, the TN content continues to increase in the AA treatments, with the AA 10 % treatment displaying the highest content of 2.94 g/Kg at day 56. Meanwhile, the AA treatments demonstrated TN levels ranging from 1.87 g/Kg to 2.38 g/Kg, compared with CK (1.38 g/Kg). All treatments showed > 1.36-fold increase in TN by day 56, with AA % treatment displaying a 2.15-fold increase. This suggests that higher AA rates may be more effective in promoting N accumulation over time, thereby highlighting an optimal AA threshold for N conservation [13].

On day 1 of composting, the initial TP levels are relatively low across all AA treatments and CK, indicating the baseline nutrient content at the start of the composting process (Fig. 6c). At day 7, compared with CK (0.210 g/Kg), TP levels in the AA treatments indicated an increasing pattern (0.240 g/Kg to 0.470 g/Kg), possibly due to organic matter decomposition and microbial mineralization [43]. Compared with CK (0.920 g/Kg), TP content continues to rise in the AA treatments (1.05 g/Kg to 1.25 g/Kg), with the AA 10 % treatment displaying the highest level of 1.40 g/Kg at day 56 of composting. At the end of composting, all AA treatments exceeded 11-fold increases; the AA 7.5 % and AA 10 % treatments yielded greater TP increases (13.9-fold to 15.6-fold). This implies that the decomposition of AA biomass releases a significant level of accumulated TP, thereby enhancing its level in the final products [16].

TK levels are relatively low across all AA treatments and CK, indicating the initial nutrient content at the start of composting (Fig. 6d). After which, the AA treatments exhibited a steady increase in TK on day 7, probably due to the rapid mineralization of organic matter and release of soluble K [43]. Compared with CK (1.94 g/Kg), TK levels continue to rise in all AA treatments (1.94 g/Kg to 2.20 g/Kg), with the AA 10 % treatment displaying the highest levels (3.21 g/Kg) at day 56 of composting. At the end of composting, the AA 10 % treatment outperformed all AA treatments (3.6-fold to 7.5-fold), with a 7.5-fold increase. This hints that higher AA rates could be more effective in promoting K accumulation over composting time [16].

The initial feedstock analysis (Table S1) confirms that AA biomass is

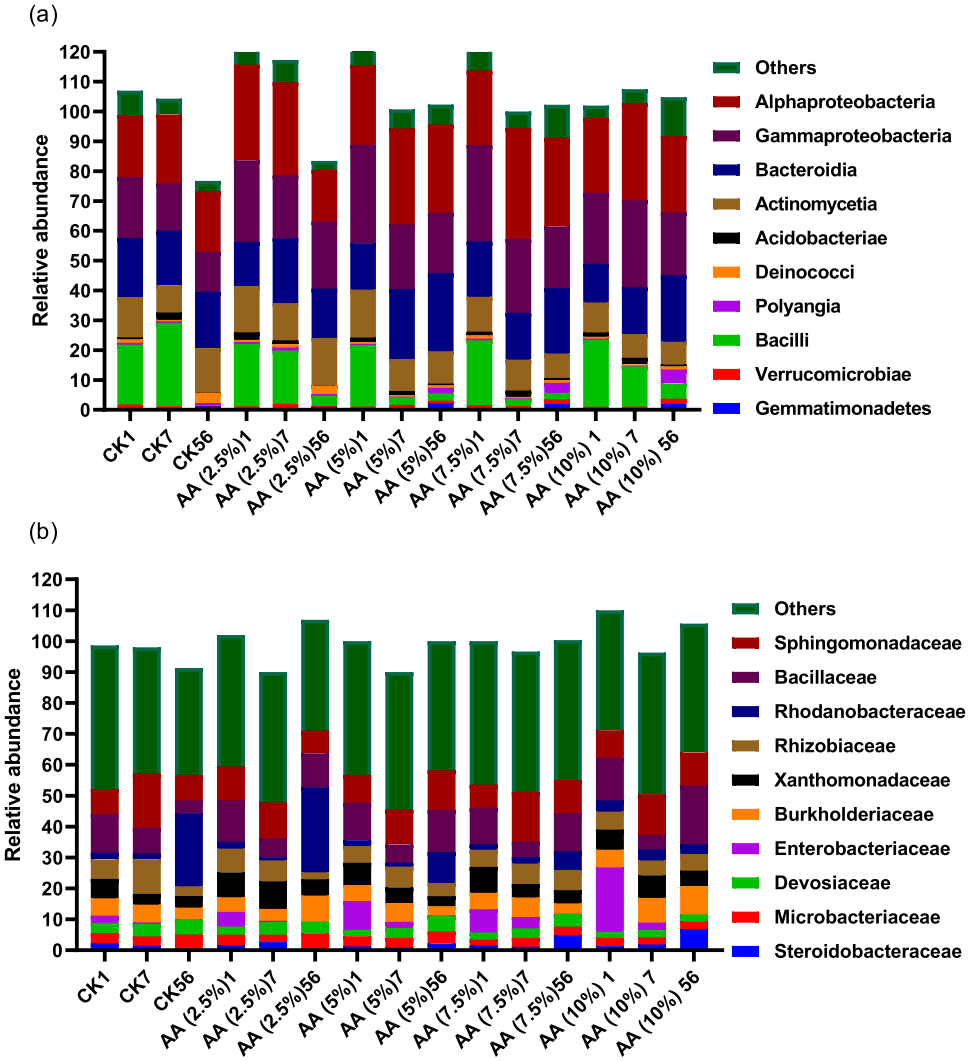

Fig. 7. Microbial community dynamics during composting, class level (a), and family level (b) during the composting process under different treatments: CK (control), AA 2.5 %, AA 5 %, AA 7.5 %, and AA 10 %. AA represents the treatment with the addition ratio of *A. adenophora*: AA 2.5 %, AA 5 %, AA 7.5 %, and AA 10 %. CK represents the control treatment of cattle manure and spent mushroom substrate.

a nutrient-rich amendment. AA contained substantial concentrations of TN (2.18 %), TP (1.25 %), and TK (1.77 %). The addition of AA at 10 % (w/w), therefore, directly introduced a significant quantity of these elements into the composting matrix. This direct input established a higher initial nutrient pool, providing the foundational basis for the observed increases in the final product. Additionally, AA chemical composition stimulated a more active microbial community that mineralized organic nutrients and, most importantly, conserved them within the stabilized compost matrix, resulting in the remarkable net retention observed.

3.5. Microbial community dynamics in response to AA application rates

Fig. 7 displays the dynamics of the microbial community structure in response to the AA application ratio at the class and family levels during composting. Alphaproteobacteria, Gammaproteobacteria, Bacteroidia, Actinomycetia, and Bacilli dominate across all treatments and stages (Fig. 7a), consistent with their known roles in organic matter decomposition through different composting phases. CK composting displays higher levels of Bacilli (20.1 %–27.9 %), Alphaproteobacteria (20.7 %–23.1 %), Gammaproteobacteria (15.8 %–20.5 %), Bacteroidia (18.3 %–19.8 %), and Actinomycetia (9.20 %–13.5 %), aligning with active degradation stages, particularly from day 1 to day 7 of composting. After which, CK exhibits lower overall diversity and a higher proportion of Alphaproteobacteria (20.3 %) on day 56, potentially reflecting microbial succession or decline of labile substrates. Meanwhile, the AA 2.5 % treatment presents elevated Alphaproteobacteria (31.2 %–32.1 %), Gammaproteobacteria (20.9 %–27.4 %), and Bacilli (17.9 %–20.9 %) early on day 1 to day 7 of composting, suggesting a stimulatory effect on nutrient-recycling microbes. However, by day 56 of composting, Gammaproteobacteria become dominant (22.5 %), suggesting stable microbial communities involved in N cycling and humification [44]. On the other hand, the AA 5 % and 7.5 % treatments maintain higher relative abundances of Alphaproteobacteria (24.9 %-37.1 %), Gammaproteobacteria (21.7 %–32.9 %), and Bacteroidia (15.6 %–23.5 %), indicative of more active decomposition processes. Actinomycetia and Bacilli persist longer, possibly enhancing cellulose and protein breakdown [44]. AA 10 % treatment exhibits the highest diversity, with a notable increase in minor classes like Polyangia, Deinococci, Acidobacteriae, and Verrucomicrobiae, possibly reflecting niche broadening due to antimicrobial compounds from AA [19]. This shift in community structure is functionally significant. The enrichment of taxa like Bacillaceae (known for antibiotic production and competitive exclusion) and Rhodanobacteraceae (versatile organic matter decomposers) under higher AA treatments (Fig. 7b) aligns with the observed suppression of pathogens and reduction in ARG hosts. This suggests that AA phytochemicals may selectively promote a microbial consortium that is both functionally robust for decomposition and antagonistic towards harmful bacteria [19,31]. Interestingly, Bacilli remain relatively abundant, possibly due to their resistance to phytochemical compounds. Finally, the composting treated with AA (AA 2.5 %, 5 %, 7.5 %, and 10 % treatments) exhibits higher microbial diversity than CK, particularly visible in the higher abundance of represented classes and evenness of distribution. CK composting (particularly in the later stage) has lower diversity and abundance in dominant microbial classes like Alphaproteobacteria and Gammaproteobacteria, suggesting reduced microbial activity or niche dominance. At the end of composting, compared with other groups, Gammaproteobacteria (2.6-fold) and Actinomycetes (2.4-fold) demonstrated the highest increases in the AA 10 % treatment, correlating with pollutant degradation and lignin degradation [44]. In comparison, AA 7.5 % treatment demonstrated a considerable increase in Bacteroidetes (1.6-fold), due to optimal organic matter availability.

Fig. 7b indicates that Bacillaceae, Microbacteriaceae, Sphingomonadaceae, and Xanthomonadaceae were the most abundant microbial families across all treatments, suggesting a shift towards more diverse, less dominant taxa as compost matures. In CK, CK1 and CK7 are characterized by high proportions of Sphingomonadaceae (8.10 %–17.5 %), Bacillaceae (8.33 %–12.5 %), and Rhizobiaceae (6.30 %–11.2 %), signifying active early- to mid-stage composting communities. CK56 shifts toward dominance by Rhodanobacteraceae (23.7 %), with a slight reduction in other families, suggesting microbial simplification and stabilization at maturity. The AA 2.5 % treatment exposes a moderate increase in Sphingomonadaceae (11.03 %–11.6 %), Bacillaceae (6.11 %–13.4 %), and Xanthomonadaceae (5.29 %–8.96 %) in the early stage of composting (1–7 days) compared to CK, which is involved in N cycling and organic compound degradation. On day 56, Bacillaceae (10.9 %) and Rhodanobacteraceae (27.6 %) still retain high abundances, denoting better preservation of functional microbial families involved in organic matter degradation. AA 5 % and AA 7.5 % treatments exhibit the most balanced and functionally rich profiles within composting. The high abundance of Bacillaceae, Rhodanobacteraceae, Rhizobiaceae, and Microbacteriaceae suggests active cellulose/protein breakdown and secondary metabolite production [44]. Both treatments display pronounced Rhodanobacteraceae and Bacillaceae on day 7 of composting, implying robust microbial activity during peak composting. By day 56, microbial families diversify, enhancing microbial succession and compost maturity.

The early stages of composting (1–7 days) in the AA 10 % treatment are strikingly different, with a significant spike in Enterobacteriaceae, known for rapid organic matter degradation and possible adaptation to phytochemical stress. This treatment also reveals elevated Devosiaceae and Steroidobacteraceae, which may reflect niche shifts or competitive dynamics induced by higher phytochemical compound levels from AA [20]. Day 56 in the AA 10 % treatment maintains higher diversity than CK, with prominent Rhodanobacteraceae, Burkholderiaceae, and Bacillaceae, implying better long-term stability and microbial richness. Finally, the AA treatments, especially 5 % and 7.5 % treatments, enhance microbial diversity and functional community structure at the family level, supporting efficient composting. The 10 % treatment, while diverse, shows a different microbial profile, potentially due to phytochemical stress selecting for resistant taxa. CK composting is less diverse and dominated by fewer families over time, suggesting less dynamic microbial succession. These findings are consistent with the work of Jiao et al. [13], who found that AA enhances the composting microbial environment by promoting copiotrophic bacteria such as Bacillaceae, Rhodanobacteraceae, and Enterobacteriaceae, all of which contribute to accelerated degradation and improved compost quality.

The observed restructuring of the microbial community (Fig. 7) in response to AA amendment was not merely a compositional change but was intrinsically linked to the enhanced functional performance of the composting system. KEGG pathway enrichment analysis of the metagenomic data provided direct genetic evidence for these functional shifts (Table S9).

The most compelling finding was the significant enrichment of pathways directly relevant to the detoxification of AA's own phytochemicals and other pollutants. Most notably, the xenobiotics biodegradation and metabolism pathway was dramatically enriched in all AA treatments at day 56, with a 3.7-fold increase in the AA 10 % treatment compared to CK. This indicates the microbial community was genetically equipped to metabolize complex organic pollutants, likely including the phenolic and terpenoid compounds derived from AA [11,13,15,19]. This is further supported by the strong enrichment in metabolism of terpenoids and polyketides (2.3-fold increase in AA 10 %), which represents a direct metabolic response to the addition of AA biomass.

Furthermore, the enrichment of pathways related to carbohydrate metabolism (2.4-fold) and amino acid metabolism (2.5-fold) indicates a community with enhanced capacity for nutrient cycling and energy production from complex organic matter. This aligns perfectly with the observed increases in enzyme activities (Fig. 5) and the higher nutrient retention (TN, TP, TK; Fig. 6) in the AA-amended composts. Concisely, the integration of taxonomic and functional gene data demonstrates that

AA amendment does not simply change who is present. Still, more importantly, it enriches a community with a genetic portfolio predisposed for efficient decomposition, xenobiotic detoxification, and competitive exclusion of pathogens, ultimately leading to the production of a stabilized and sanitized compost product.

3.6. Impact of AA application ratios on functional gene composition during composting

Additives like plant residues can alter the microbial community composition and succession, affecting the gene functions expressed at different stages of composting [45]. AA treatments and CK exhibited significantly different compositions of GO, with considerable differences between the composting stages (Fig. 8). Fig. 8a indicates that the relative abundance of genes associated with cellular components generally increases with the application of AA. CK (CK1, CK7, and CK56) displays the lowest abundance, ranging from 0.0184 % to 0.0547 %. As the ratio of AA increases, there is a noticeable increase in the relative abundance, with the highest abundance (0.183 %) observed in the AA10 % treatment on day 56, suggesting that adding AA might enhance the complexity or diversity of cellular structures involved in composting [19]. Meanwhile, the biological processes display a similar trend during composting. CK has a lower abundance (0.084–0.277 %), with the highest being 0.277 % noted on day 56 of composting. As the ratio of AA increases, the relative abundance also increases, peaking at 0.487 % on day 56 of AA 10 % treatment. Adding AA may stimulate more active and diverse biological processes during composting [46]. In terms of molecular functions, CK again displays lower abundances, with the highest being 0.341 % on day 7, then reduced to 0.209 % on day 56. Adding AA increases the relative abundance of genes associated with molecular functions, with the highest abundance of 0.596 % observed on day 56 of AA 10 % treatment. This suggests that AA application might boost the variety of molecular functions or the efficiency of specific molecular processes during composting [15].

From day 1 to day 7 of composting, compared with CK, AA treatments showed a decrease in GO level 1 abundance, probably due to the transition from mesophilic to thermophilic phases, which temporarily suppresses gene expression [39] along with the effect of phytochemicals. From day 7 to day 56, AA treatments demonstrated recovery and an increase in GO terms, especially at higher rates, highlighting AA's role in sustaining microbial activity [16]. By the end of the composting process, the AA treatments (AA 2.5 % to AA 10 %) experienced more than a 2.5-fold increase in the molecular function, linked to compost-induced microbial enzyme production. The AA 10 % treatment illustrated the highest increases in molecular function (4.43-fold), biological process (1.60-fold), and cellular component (10.2-fold), indicating enhanced structural and enzymatic activity.

Fig. 8b shows the dynamics of GO level 2 during composting under the AA application impact. Catalytic activity (GO:0003824), transporter activity (GO:0005215), structural molecule activity (GO:0005198), and antioxidant activity (GO:0016209) consistently dominate the AA treatments and CK, suggesting these processes are critical for composting, especially in the AA treatments. Compared with other treatments, GO:0003824 abundance peaks on day 7 and day 56 of composting in the AA 5 % and AA 10 % treatments, respectively. Increasing GO:0003824 abundance reflects enhanced enzymatic degradation of complex organics. This enrichment in functional genetic potential, particularly in molecular functions related to catalytic activity (GO:0003824) (Fig. 8b), provides a genetic basis for the observed enhancements in enzyme activities (Fig. 5) and pollutant removal. The stimulated microbial community appears better equipped to decompose complex organics, including the phytochemicals themselves, and immobilize heavy metals [19]. Enzymes such as cellulases, amylases, and proteases catalyze the decomposition of cellulose, starches, and proteins, respectively, facilitating the conversion of organic waste into simpler compounds and humic substances [37]. The abundance of GO:0005215 was considerably enhanced on days 1 and 7 of composting in the AA 5 % and AA 10 % treatments, indicating increased activity in the directed movement of substances such as nutrients, ions, and small molecules across microbial cell membranes during composting. This transporter activity supports nutrient uptake and waste removal in microbial communities, which is critical for efficient decomposition and microbial metabolism [47]. GO:0005198 abundance increases slightly over time in AA treatments, notably the AA 7.5 % and AA 10 % treatments. GO:0005198 activity involves molecules that provide structural integrity to cells or cellular components. Structural molecules help maintain cell shape and stability in composting microbes, supporting microbial growth and function under varying environmental conditions [48]. Compared with CK, notable increases in GO:0016209 abundance were noted in AA treatments, especially on day 1 and day 56 of composting in the AA 10 % treatment. The rise in GO:0016209 abundance implies microbial stress adaptation mechanisms, possibly responding to oxidative stress from rapid organic breakdown [49].

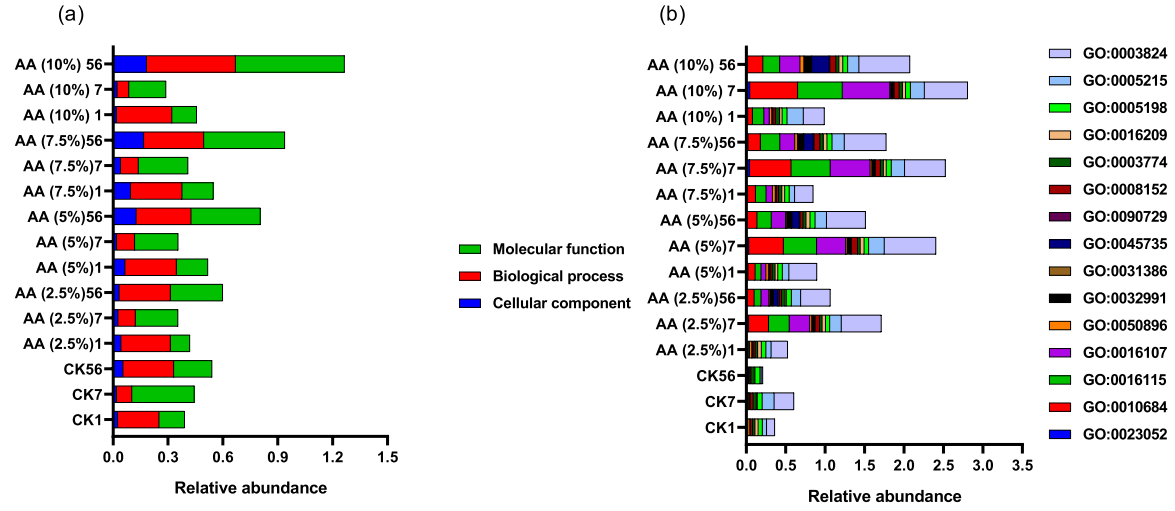

Fig. 8. Gene ontology (GO) dynamics during composting, GO level 1 (a), and GO level 2 (b) during the composting process under different treatments: CK (control), AA 2.5 %, AA 5 %, AA 7.5 %, and AA 10 %. AA represents the treatment with the addition ratio of *A. adenophora*: AA 2.5 %, AA 5 %, AA 7.5 %, and AA 10 %. CK represents the control treatment of cattle manure and spent mushroom substrate.

3.7. Impact of AA application ratios on carbohydrate-active enzymes dynamics during composting

Carbohydrate-active enzymes (CAZymes) are essential biomarkers for microbial functional capacity in composting ecosystems, particularly reflecting microbial roles in organic matter decomposition. To explore how AA affects microbial functionality, the relative abundance of CAZyme classes was analyzed over time in composts mixed with increasing AA rates (2.5 %, 5 %, 7.5 %, 10 %) compared with CK (Fig. 9). Across all treatments, glycoside hydrolases (GHs), glycosyl transferases (GTs), and carbohydrate-binding modules (CBMs) consistently emerged as the most abundant CAZyme classes, reflecting their central roles in organic matter degradation in the composting (Fig. 8a). For example, on day 1 in CK, GHs dominated with a relative abundance of 0.463, followed by GTs (0.231) and CBMs (0.126). Similar patterns were seen in AA-amended groups, indicating that core CAZyme profiles were maintained despite treatment variations. Lignocellulose additives promote the secretion and abundance of CAZymes such as GHs, GTs, and CBMs that degrade cellulose, hemicellulose, and lignin more efficiently [38].

During the early composting stage (day 1), AA treatments slightly increased GH and GT abundance compared to the CK. For example, on day 1, the abundance of GHs in the AA 2.5 % treatment was 0.464 compared with CK (0.463). Meanwhile, the abundance of GTs in the AA 2.5 % treatment was 0.232 compared with CK (0.231). A shift in CAZyme composition was observed across all treatments, with a slight decline in GHs and GTs by day 56, possibly reflecting the depletion of easily degradable carbohydrates and a transition toward more recalcitrant organic matter. GHs decreased from 0.463 (CK1) to 0.440 (CK56), and GTs from 0.231 (CK1) to 0.220 (CK56). Similar trends appeared in AA treatments. In the AA 10 % treatment, GHs fell from 0.468 (on day 1) to 0.452 (on day 56), and GTs from 0.235 (on day 1) to 0.227 (on day 56). Despite these drops, the higher level of GH and GT in the AA 10 % treatment at day 56 compared to CK55 suggests that AA may help maintain microbial carbohydrate-degrading potential during later stages of composting [36].

Auxiliary activities (AAs) showed marginal increases in composting, particularly under the AA treatments. For example, on day 1, the abundance in the AA10 % treatment was 0.056 vs. CK1: 0.054. And on day 56, the abundance in the AA 10 % treatment was 0.0589 vs. CK56: 0.056. This could be linked to oxidative enzymes involved in lignin degradation, suggesting a potential ligninolytic effect of AA addition [38]. Carbohydrate esterases (CEs) also increased modestly over time, particularly on day 56 in the AA 10 % treatment (0.052) compared to CK56 (0.051), indicating enhanced deacetylation and side-chain cleavage activity as composting progressed [36]. Although composting time was the main driver of CAZyme dynamics, higher AA application ratios in the 7.5 % and 10 % treatments appeared to enrich GT (8.81-fold and 1.27-fold), GH (8.81-fold and 1.27-fold), CBM (1.81-fold and 2.68-fold), CE (1.95-fold and 3.91-fold), AA (18.3-fold and 21.8-fold), and PL (1.76-fold and 2.71-fold) abundance and diversity modestly, especially in later stages, due to AA's rich content in complex plant polymers, stimulating a broader spectrum of microbial enzymatic capabilities [16].

Also, the effect of AA application on the family-level dynamics of CAZymes during composting was explored. The analysis focuses on 16 CAZyme families with the highest functional contributions, across composting days 1, 7, and 56, for the AA treatments (2.5 %, 5 %, 7.5 %, and 10 %) and CK (Fig. 9b). The overall CAZyme family abundance declined over time in the CK (from 0.520 at CK1–0.332 at CK56), reflecting a natural reduction in microbial enzymatic activity as labile substrates were depleted. In contrast, the AA treatments, particularly at the higher rates (7.5 % and 10 % treatments), retained significantly higher total CAZyme levels by day 56 as follows: 1.10, 0.692, 0.717, and 0.616 in AA 10 %, AA 7.5 %, AA 5 %, and AA 2.5 %, respectively. This pattern suggests that AA application, especially at $\geq$ 5 %, helps maintain microbial functional potential in later composting stages [16].

3.8. Relationships among phytochemicals, physicochemical properties, enzymes, pathogens, functional genes, and heavy metal availability

Fig. 10 elucidates the complex interconnections among compost characteristics, including phytochemical dynamics, physicochemical parameters, enzyme activities, pathogen abundance, GO level 1 functional profiles, and heavy metal availability, using Mantel tests and Spearman's correlation analysis. Fig. 10a exhibits that the strongest associations (Mantel's $|r| \geq 0.4$, thick lines) were observed primarily between HHO and microbial, enzymatic, and heavy metal bioavailability parameters. DTD and HHO showed comprehensive connectivity, implying their central regulatory roles in composting biochemical

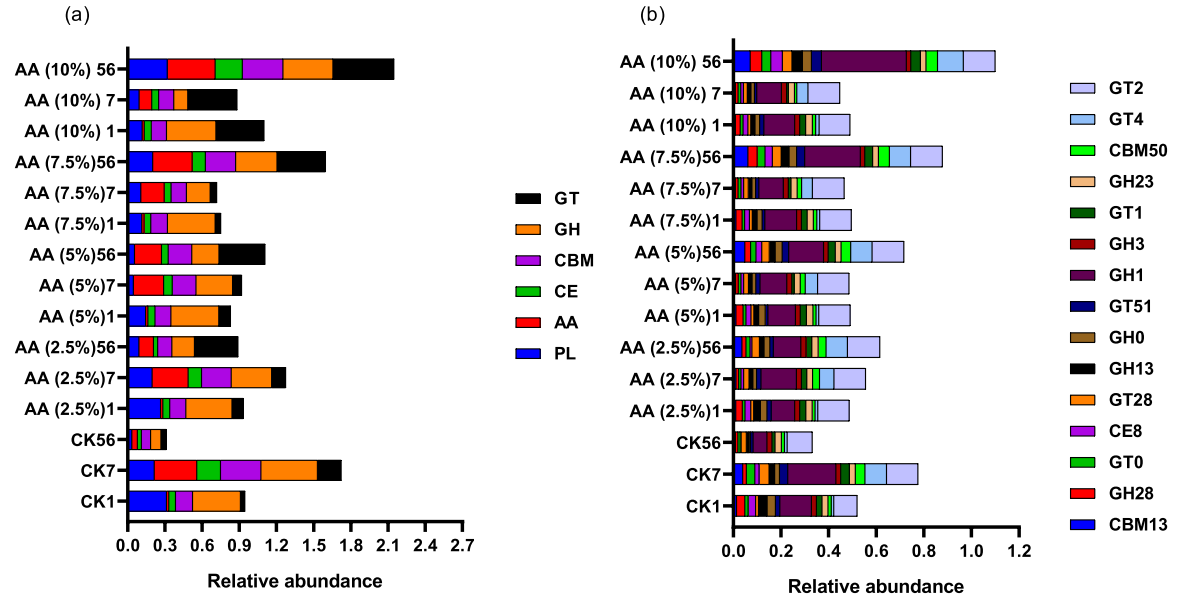

Fig. 9. CAZymes dynamics during composting, CAZymes class (a), and CAZymes family (b) during the composting process under different treatments: CK (control), AA 2.5 %, AA 5 %, AA 7.5 %, and AA 10 %. AA represents *A. adenophora* additive. AA represents the treatment with the addition ratio of *A. adenophora*: AA 2.5 %, AA 5 %, AA 7.5 %, and AA 10 %. CK represents the control treatment of cattle manure and spent mushroom substrate.

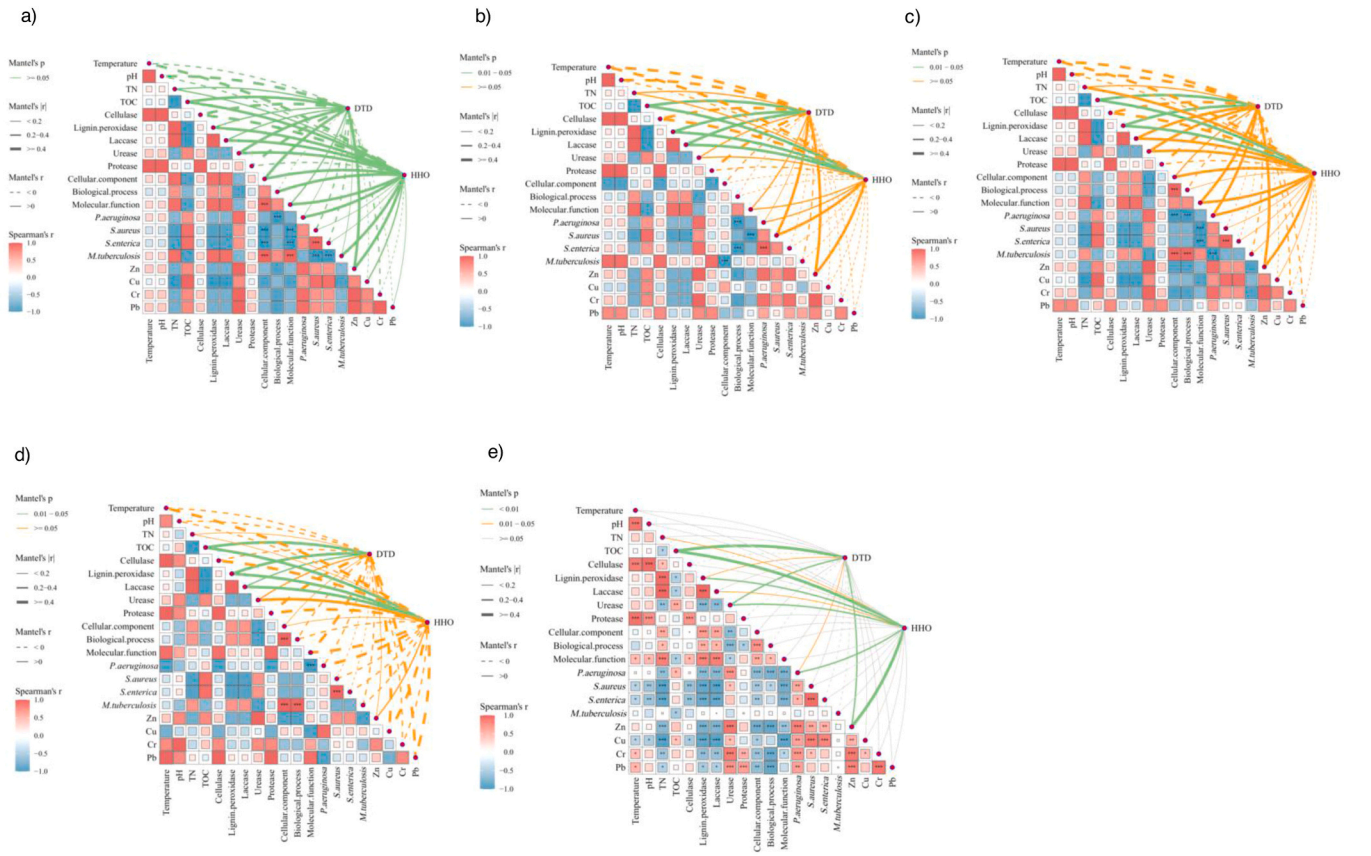

Fig. 10. Relationships among phytochemicals, physicochemical properties, enzymes, pathogens, GO level 1, and heavy metal availability using the Mantel test. a) CK group; b) 2.5 % treatment; c) 5 % treatment; d) 7.5 % treatment; and e) 10 % treatment. The significance levels are: *p < 0.05, **p < 0.01, ***p < 0.001.

processes. Pathogens (*P. aeruginosa*, *S. aureus*, *S. enterica*, *M. tuberculosis*) exhibited negative correlations with enzyme activities and GO categories (Spearman's r ≈ −0.3 to −0.7), significant at $p < 0.001$. This indicates that higher enzymatic and microbial functional activity corresponds to pathogen suppression, a critical finding for compost sanitation [50]. The HHO and DTD were also negatively associated with pathogen abundances, suggesting a direct or indirect antimicrobial effect of these phytochemicals, possibly via modulation of microbial consortia or enzyme stimulation [50,51]. The bioavailability of heavy metals (Zn, Cu, Cr, and Pb) displayed negative correlations with enzymes, GO categories, and physicochemical factors. Higher enzyme activities and microbial functional richness correlate with lower heavy metal bioavailability, potentially due to mechanisms such as biosorption, complexation with microbial metabolites, and formation of stable organic-metal complexes [52,53]. Fig. 10 b displays that cellulase, laccase, lignin peroxidase, urease, and protease are positively associated with HHO, with Mantel's r often ≥ 0.4. These enzymes are critical for organic matter decomposition and nutrient cycling. The stimulation of enzymatic activity by HHO may result from direct microbial stimulation (growth or gene expression), indirect effects via shifts in community structure, or potential synergistic interactions among phytochemical compounds [54]. Significant positive associations were observed between phytochemicals, particularly HHO, and all three GO categories. These correlations suggest that phytochemical input enriches microbial functional diversity and capacity, which aligns with increased enzymatic activity and biodegradation potential [55]. Pathogens such as *P. aeruginosa*, *S. aureus*, *S. enterica*, and *M. tuberculosis* were negatively correlated with enzymes and GO terms (Spearman $r < -0.3$ to −0.7, $p < 0.001$). HHO also had negative Mantel correlations with pathogens, though not always statistically significant at the 0.01 level (dashed orange lines). This suggests that increased enzymatic and microbial functional activity contributes to pathogen suppression, essential for achieving hygienically safe compost [50,56]. Zn, Cu, Cr, and Pb were negatively correlated with enzyme activity and microbial functions. Notably, strong Spearman's r values (often <−0.4) indicated that higher enzymatic and microbial activity coincided with lower bioavailability of heavy metals. Meanwhile, HHO demonstrated strong Mantel correlations (r ≥ 0.4) with heavy metal dynamics, underscoring its role in driving detoxification pathways [57]. Fig. 10c shows that both HHO and DTD are positively associated with core composting parameters. TN, temperature, and pH showed positive Mantel correlations. These parameters are crucial for maintaining microbial activity and optimal composting kinetics [58]. The phytochemicals enhance nutrient retention and thermal stabilization by influencing microbial metabolism and matrix structure [54]. GO categories, cellular component, biological process, and molecular function, showed strong positive correlations with both phytochemicals. These relationships suggest expanding microbial metabolic and cellular capabilities, aligning with previous observations of phytochemicals fostering diverse and active microbiomes [56]. *P. aeruginosa, S. aureus, S. enterica*, and *M. tuberculosis* were negatively correlated with enzyme activities and GO terms. The strongest suppressive effects ($p < 0.001$) were observed for urease and protease, particularly against *P. aeruginosa* and *S. enterica*. Mantel test results show mostly dashed edges between HHO and pathogens, reinforcing an inverse relationship. This suggests that enhanced microbial functionality suppresses pathogens, potentially through competitive exclusion, production of antimicrobial metabolites, and accelerated organic matter stabilization (which limits pathogen niches) [50,56]. Phytochemicals, especially HHO, indirectly contribute to compost sanitization and safety through this pathway. Zn, Cu, Cr, and Pb were negatively correlated with microbial enzymes and GO terms (blue heatmap cells). Strongest negative correlations were seen with Cr and Pb

across several biological parameters. HHO in particular showed negative Mantel correlations with heavy metal bioavailability, implying a role in detoxification [57]. Fig. 10d displayed that both HHO and DTD were positively correlated with essential physicochemical indicators of compost health, probably because AA creates favorable environmental conditions for microbial processes and buffers compost systems to maintain optimal thermophilic activity and nutrient retention [54,58]. Temperature, pH, and TN exhibited moderate to strong Mantel correlations ($r \geq 0.4$) with phytochemicals. These properties are directly tied to microbial activity and degradation dynamics [18]. HHO had high Mantel r values (≥ 0.4) and Spearman's $r \geq 0.6$ with cellulase, lignin peroxidase, laccase, urease, and protease. These enzymes are fundamental to organic matter decomposition, including lignocellulosic breakdown and N turnover. *P. aeruginosa*, *S. aureus*, *S. enterica*, and *M. tuberculosis* exhibited strong negative Spearman correlations ($r < -0.5$, $p < 0.001$) with enzymes and GO terms. Phytochemicals also maintained negative Mantel correlations with these pathogens. This pattern suggests indirect suppression mechanisms such as competitive exclusion by beneficial microbes, antimicrobial by-products of enzymatic degradation, and faster degradation, reducing favorable niches for pathogens [50,56]. Zn, Cu, Cr, and Pb bioavailability displayed negative associations with enzymes, GO terms, and phytochemicals. Notably, Pb and Cr exhibited some of the strongest negative Spearman r values ($r < -0.5$), and HHO had thick dashed orange edges, indicating substantial negative Mantel correlations with these metals. The possible mechanisms may include microbial biosorption of metals due to increased biomass, organic complexation via phenolic and flavonoid structures, and enzyme-facilitated humification, which immobilizes metals [26].

Fig. 10e shows that *P. aeruginosa*, *S. aureus*, *S. enterica*, and *M. tuberculosis* have strongly negative Spearman's correlations with enzymes and GO terms (blue cells, $p < 0.001$). Dashed Mantel edges to HHO are particularly strong in *P. aeruginosa* and *S. enterica*. This suggests an apparent antagonistic effect of microbial functional enhancement on pathogen persistence, probably mediated by competitive exclusion, antimicrobial enzyme by-products (such as laccase, peroxidase), or environmental changes (temperature, pH) unfavorable to pathogen survival [56,58]. Zn, Cu, Cr, and Pb are negatively associated with phytochemical-induced activity. Cr and Pb exhibit particularly strong inverse relationships with enzymes and GO functions in both Spearman and Mantel analyses. Dashed Mantel lines from HHO to heavy metal bioavailability suggest a significant negative correlation ($p < 0.05$) and a substantial effect size. These patterns imply that phytochemical stimulation leads to lower heavy metal bioavailability, possibly due to complexation with polyphenolic compounds or incorporation into stabilized humic structures facilitated by enzymatic activity [5,59]. Finally, these outcomes suggest that composting amended with AA reduces phytotoxic phytochemicals, enhances beneficial enzyme activities and microbial diversity, decreases pathogens, modulates functional genes related to nutrient cycling, and decreases heavy metal availability through interactions among organic matter, microbes, and environmental factors, thereby producing a quality compost product (Fig. 11).

Although this study demonstrates the significant benefits of the AA amendment in composting, certain limitations and future research directions should be acknowledged. The precise contributions of specific phytochemicals versus the overall microbial response remain to be fully disentangled; future work could involve controlled incubations with purified DTD/HHO. Furthermore, the long-term stability of the immobilized heavy metals and the persistence of pathogen suppression in soil amended with AA-compost should be verified through pot and field trials. A direct comparative assessment with traditional amendments like biochar would also be valuable to fully quantify the economic and ecological advantages of using AA. Finally, qPCR validation of key ARGs would strengthen the metagenomic findings. Despite these areas for further study, our results robustly indicate that AA can be effectively valorized from a problematic invasive species into a high-value compost amendment that simultaneously addresses multiple aspects of compost safety and quality.

4. Conclusions

Integrating *Ageratina adenophora* (AA) into composting significantly influences pollutant behavior, pathogen control, and microbial activity. Using higher amounts of AA (7.5 % and 10 %) enhances heavy metal immobilization and reduces bioavailability, thus lowering environmental risks from metal toxicity. These levels also suppress harmful microorganisms and antibiotic resistance genes, showcasing AA's ability to improve compost sanitation. Additionally, AA amendments boost enzyme activities, especially those involved in breaking down lignin and cellulose, which promotes efficient organic matter decomposition. The resulting composts feature greater microbial diversity, fostering stable, functional microbial communities during maturation. Overall, these

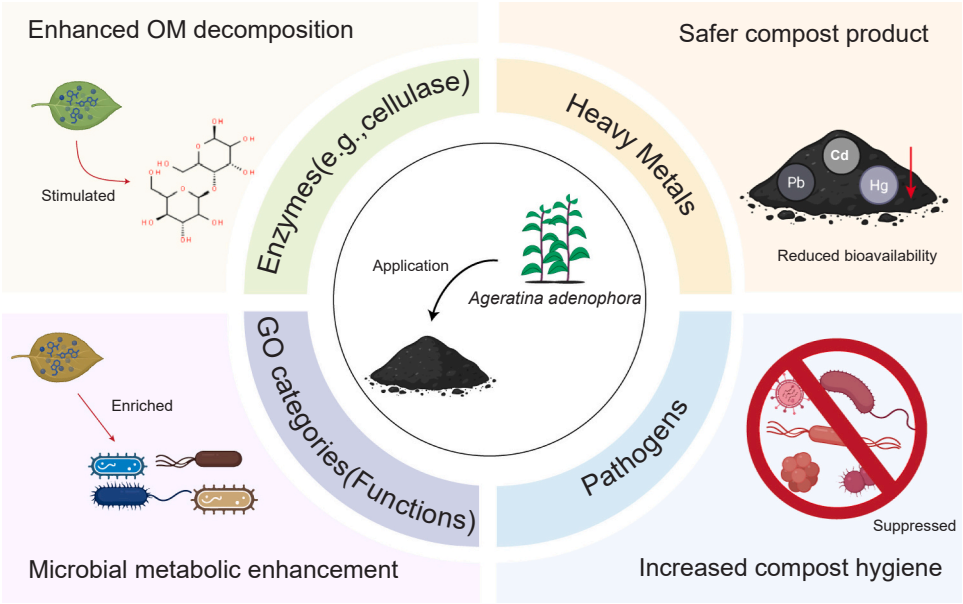

Fig. 11. Conceptual diagram illustrating that AA application significantly impacts pathogens, pollutants, and metabolic functions during the composting process.

findings highlight AA's potential in optimizing composting for sustainable waste management and safe agricultural use. However, further research is necessary to evaluate the long-term ecological risks of AA-derived compost, especially its possible invasiveness. Future studies should also compare AA with other traditional amendments like biochar and humic acid to better understand its relative advantages in composting systems.

Environmental implication

This study demonstrates the dual potential of *Ageratina adenophora* (AA), an invasive species, to enhance compost quality while mitigating environmental hazards. Its phytochemical properties significantly reduced the bioavailability of heavy metals, pathogenic loads, and antibiotic resistance genes, thereby lowering the ecological and health risks associated with composting organic waste. Converting problematic biomass into a functional bioremediation agent offers a sustainable, low-cost solution for waste management and soil restoration. Implementing AA in composting systems supports circular economy strategies and presents a scalable alternative for managing both invasive plant species and contaminated organic waste streams.

CRediT authorship contribution statement

Yousif Abdelrahman Yousif Abdellah: Writing – review & editing, Writing – original draft, Resources, Methodology, Formal analysis, Data curation, Conceptualization. **Jianou Gao:** Visualization, Software. **Dou Tingting:** Visualization, Software. **Zhenyan Yang:** Resources, Project administration. **Shimei Yang:** Resources, Methodology. **Ayodeji Bello:** Writing – review & editing, Writing – original draft. **Chengmo Yang:** Resources, Project administration. **Dong Liu:** Writing – review & editing, Writing – original draft, Supervision. **Elsheikh Elsiddig A. E.:** Writing – review & editing, Writing – original draft. **Fuqiang Yu:** Writing – review & editing, Supervision, Project administration.

Declaration of Competing Interest

The authors declare that they have no known competing financial interests or personal relationships that could have appeared to influence the work reported in this paper.

Acknowledgments

This research was funded by the Caiyun Postdoctoral Project of Yunnan Province, the Yunnan Key Project of Science and Technology (202402AE090030), the Yunnan Revitalization Talent Support Program to Dong Liu, and the Yunnan Technology Innovation Program (202205AD160036).

Appendix A. Supporting information

Supplementary data associated with this article can be found in the online version at doi:10.1016/j.jhazmat.2025.140404.

Data availability

Data will be made available on request.

References

[1] Chen, Z., Xing, R., Yang, X., Zhao, Z., Liao, H., Zhou, S., 2021. Enhanced in situ Pb (II) passivation by biotransformation into chloropyromorphite during sludge composting. J Hazard Mater 408, 124973. https://doi.org/10.1016/j.jhazmat.2020.124973.

[2] Tchounwou, P.B., Yedjou, C.G., Patlolla, A.K., Sutton, D.J., 2012. Heavy Metal Toxicity and the Environment BT-molecular, clinical and environmental toxicology. In: Luch, A. (Ed.), Environmental Toxicology, 3. Springer, Basel, Basel, pp. 133–164. https://doi.org/10.1007/978-3-7643-8340-4_6.

[3] Barathe, P., Kaur, K., Reddy, S., Shriram, V., Kumar, V., 2024. Antibiotic pollution and associated antimicrobial resistance in the environment. J Hazard Mater Lett 5, 100105. https://doi.org/10.1016/j.hazl.2024.100105.

[4] Browne, S., Bhatia, S., Sarkar, N., Kaushik, M., 2023. In: Singh, P., of A, M.B.T.-D., from V.S. Sillanpää, A.-R.B. (Eds.), Chapter 11 - Antibiotic-resistant bacteria and antibiotic-resistant genes in agriculture: a rising alarm for future. Dev. Microbiol., Academic Press, pp. 247–274. https://doi.org/10.1016/B978-0-323-99866-6.00017-9.

[5] Abdellah, Y.A.Y., Chen, H.-Y., Deng, S.-W., Li, W.-T., Ren, R.-J., Yang, X., Rana, M. S., Sun, S.-S., Liu, J.-J., Wang, R.-L., 2024. *Mikania micrantha* Kunth and its derived biochar impacts on heavy metal bioavailability and siderophore-related genes during chicken manure composting. Biochar 6, 56. https://doi.org/10.1007/s42773-024-00347-w.

[6] Sun, S., Abdellah, Y.A.Y., Miao, L., Wu, B., Ma, T., Wang, Y., Zang, H., Zhao, X., Li, C., 2022. Impact of microbial inoculants combined with humic acid on the fate of estrogens during pig manure composting under low-temperature conditions. J Hazard Mater 424, 127713. https://doi.org/10.1016/j.jhazmat.2021.127713.

[7] Tran, H.-T., Bolan, N., Lin, C., Binh, Q., Nguyen, M.-K., Luu, T.A., Le, V., Pham, C., Hoang, H., Vo, D., 2023. Succession of biochar addition for soil amendment and contaminants remediation during co-composting: a state of art review. J Environ Manag 342, 118191. https://doi.org/10.1016/j.jenvman.2023.118191.

[8] Dang, Q., Zhao, X., Yang, T., Gong, T., He, X., Tan, W., Xi, B., 2022. Coordination of bacterial biomarkers with the dominant microbes enhances triclosan biodegradation in soil amended with food waste compost and cow dung compost. Sci Total Environ, 153837. https://doi.org/10.1016/j.scitotenv.2022.153837.

[9] Jiang, Z., Li, X., Li, M., Zhu, Q., Li, G., Ma, C., Li, Q., Meng, J., Liu, Y., Li, Q., 2021. Impacts of red mud on lignin depolymerization and humic substance formation mediated by laccase-producing bacterial community during composting. J Hazard Mater 410, 124557. https://doi.org/10.1016/j.jhazmat.2020.124557.

[10] Niedrite, E., Klavins, L., Dobkevica, L., Purmalis, O., Ievinsh, G., Klavins, M., 2024. Sustainable control of invasive plants: Compost production, quality and effects on wheat germination. J Environ Manag 371, 123149. https://doi.org/10.1016/j.jenvman.2024.123149.

[11] Abdellah, Y.A.Y., Liu, D., Tingting, D., Gao, J., Yang, S., Yang, Z., Yang, C., Elsheikh, E.A.E., Sun, S., Bello, A., Yu, F., 2025. Composting *Ageratina adenophora* with spent mushroom substrate: phytochemical degradation, greenhouse gas mitigation, and enhanced nutrient cycling. J Environ Chem Eng 13, 118776. https://doi.org/10.1016/j.jece.2025.118776.

[12] Udume, O.A., Abu, G.O., Stanley, H.O., Vincent-Akpu, I.F., Momoh, Y., 2022. Impact of composting factors on the biodegradation of lignin in *Eichhornia crassipes* (water hyacinth): a response surface methodological (RSM) investigation. Heliyon 8, e10340. https://doi.org/10.1016/j.heliyon.2022.e10340.

[13] Jiao, Y., Li, Y., Yuan, L., Huang, J., 2021. Allelopathy of uncomposted and composted invasive aster (*Ageratina adenophora*) on ryegrass. J Hazard Mater 402, 123727. https://doi.org/10.1016/j.jhazmat.2020.123727.

[14] Liu, H., Zhao, Q., Cheng, Y., 2022. Composted invasive plant *Ageratina adenophora* enhanced barley (Hordeum vulgare) growth and soil conditions. PLoS One 17, e0275302. https://doi.org/10.1371/journal.pone.0275302.

[15] Jiao, Y., Jia, R., Sun, Y., Yang, G., Li, Y., Huang, J., Yuan, L., 2021. In situ aerobic composting eliminates the toxicity of *Ageratina adenophora* to maize and converts it into a plant- and soil-friendly organic fertilizer. J Hazard Mater 410, 124554. https://doi.org/10.1016/j.jhazmat.2020.124554.

[16] Zhao, M., Lu, X., Zhao, H., Yang, Y., Hale, L., Gao, Q., Liu, W., Guo, J., Li, Q., Zhou, J., Wan, F., 2019. *Ageratina adenophora* invasions are associated with microbially mediated differences in biogeochemical cycles. Sci Total Environ 677, 47–56. https://doi.org/10.1016/j.scitotenv.2019.04.330.

[17] Giri, S., Sahu, R., Paul, P., Nandi, G., Dua, T.K., 2022. An updated review on *Eupatorium adenophorum* Spreng. [*Ageratina adenophora* (Spreng.)]: traditional uses, phytochemistry, pharmacological activities and toxicity. Pharmacol Res Mod Chin Med 2, 100068. https://doi.org/10.1016/j.prmcm.2022.100068.

[18] Abdellah, Y.A.Y., Luo, Y.-S., Sun, S.-S., Yang, X., Ji, H.-Y., Wang, R.-L., 2023. Phytochemical and underlying mechanism of *Mikania micrantha* Kunth on antibiotic resistance genes, and pathogenic microbes during chicken manure composting. Bioresour Technol 367, 128241. https://doi.org/10.1016/j.biortech.2022.128241.

[19] Parsiaaref, S., Cao, A., Li, Y., Ebadollahi, A., Parmoon, G., Gholamnezhad, J., Wang, Q., Yan, D., Fang, W., Song, Z., Wang, X., Zhang, M., 2024. Studying the antifungal effects of *Ageratina adenophora* (Sprengel) R. King and H. Robinson (=*Eupatorium adenophorum* Sprengel) as a Bio-fumigant plant alone and in combination with biochar against *Pythium aphanidermatum* (Edson) Fitz. Plants 13. https://doi.org/10.3390/plants13243511.

[20] Xu, R., Weng, J., Hu, L., Peng, G., Ren, Z., Deng, J., Jia, Y., Wang, C., He, H., Hu, Y., 2018. Anti-NDV activity of 9-oxo10,11-dehydroageraphorone extracted from *Eupatorium adenophorum* Spreng in vitro. Nat Prod Res 32, 2244–2247. https://doi.org/10.1080/14786419.2017.1371158.

[21] Fu, T., Shen, C., Mi, H., Tang, J., Li, L., Lin, H., Shangguan, H., Yu, Z., 2025. Alternating electric field as an effective inhibitor of bioavailability and phytotoxicity of heavy metals during electric field-assisted aerobic composting. J Hazard Mater 490, 137842. https://doi.org/10.1016/j.jhazmat.2025.137842.

[22] Liu, Q., He, X., Wang, K., Li, D., 2023. Biochar drives humus formation during composting by regulating the specialized metabolic features of microbiome. Chem Eng J 458, 141380. https://doi.org/10.1016/j.cej.2023.141380.

[23] Liu, X., Li, H., Yang, J., Yan, S., Zhou, Y., Jiang, R., Li, R., Wang, M., Ren, P., 2025. Different effects of bio/non-degradable microplastics on sewage sludge compost

performance: Focusing on antibiotic resistance genes, virulence factors, and key metabolic functions. J Hazard Mater 488, 137329. https://doi.org/10.1016/j.jhazmat.2025.137329.
[24] Yousif Abdellah, Y.A., Shi, Z.-J., Luo, Y.-S., Hou, W.-T., Yang, X., Wang, R.-L., 2022. Effects of different additives and aerobic composting factors on heavy metal bioavailability reduction and compost parameters: a meta-analysis. Environ Pollut 307, 119549. https://doi.org/10.1016/j.envpol.2022.119549.
[25] Guo, H., Liu, H., Wu, S., 2022. Immobilization pathways of heavy metals in composting: Interactions of microbial community and functional gene under varying C/N ratios and bulking agents. J Hazard Mater 426, 128103. https://doi.org/10.1016/j.jhazmat.2021.128103.
[26] Lin, H., Liu, C., Li, B., Dong, Y., 2021. Trifolium repens L. regulated phytoremediation of heavy metal contaminated soil by promoting soil enzyme activities and beneficial rhizosphere associated microorganisms. J Hazard Mater 402, 123829. https://doi.org/10.1016/j.jhazmat.2020.123829.
[27] Xia, X., Wu, S., Zhou, Z., Wang, G., 2021. Microbial Cd(II) and Cr(VI) resistance mechanisms and application in bioremediation. J Hazard Mater 401, 123685. https://doi.org/10.1016/j.jhazmat.2020.123685.
[28] Singh, R., Dong, H., Liu, D., Zhao, L., Marts, A.R., Farquhar, E., Tierney, D.L., Almquist, C.B., Briggs, B.R., 2015. Reduction of hexavalent chromium by the thermophilic methanogen *Methanothermobacter thermautotrophicus*. Geochim Cosmochim Acta 148, 442–456. https://doi.org/10.1016/j.gca.2014.10.012.
[29] Long, Y., Zhu, N., Zhu, Y., Shan, C., Jin, H., Cao, Y., 2024. Hydrochar drives reduction in bioavailability of heavy metals during composting via promoting humification and microbial community evolution. Bioresour Technol 395, 130335. https://doi.org/10.1016/j.biortech.2024.130335.
[30] Song, C., Zhao, Y., Pan, D., Wang, S., Wu, D., Wang, L., Hao, J., Wei, Z., 2021. Heavy metals passivation driven by the interaction of organic fractions and functional bacteria during biochar/montmorillonite-amended composting. Bioresour Technol 329, 124923. https://doi.org/10.1016/j.biortech.2021.124923.
[31] Niu, Q., Li, K., Yang, H., Zhu, P., Huang, Y., Wang, Y., Li, X., Li, Q., 2022. Exploring the effects of heavy metal passivation under Fenton-like reaction on the removal of antibiotic resistance genes during composting. Bioresour Technol 359, 127476. https://doi.org/10.1016/j.biortech.2022.127476.
[32] Su, Q., Wu, Y., Wang, S., Li, Y., Zhao, J., Huang, F., Wu, J., 2023. The reverse function of lignin-degrading enzymes: the polymerization ability to promote the formation of humic substances in domesticated composting. Bioresour Technol 380, 129059. https://doi.org/10.1016/j.biortech.2023.129059.
[33] Abdellah, Y.A.Y., Yang, S., Yang, C., Yang, Z., Elsheikh, E.A.E., Keiblinger, K.M., Mohamed, T.A., Rana, M.S., Liu, D., Yu, F., 2025. Tobacco waste valorization through composting: a systematic review of biomass conversion efficiency and circular bioeconomy strategies. Biomass Bioenergy 201, 108137. https://doi.org/10.1016/j.biombioe.2025.108137.
[34] Hemati, A., Aliasgharzad, N., Khakvar, R., Khoshmanzar, E., Asgari Lajayer, B., van Hullebusch, E.D., 2021. Role of lignin and thermophilic lignocellulolytic bacteria in the evolution of humification indices and enzymatic activities during compost production. Waste Manag 119, 122–134. https://doi.org/10.1016/j.wasman.2020.09.042.
[35] Hilgers, R., Vincken, J.-P., Gruppen, H., Kabel, M.A., 2018. Laccase/mediator systems: their reactivity toward phenolic lignin structures. ACS Sustain Chem Eng 6, 2037–2046. https://doi.org/10.1021/acssuschemeng.7b03451.
[36] He, Y., Lin, R., Yu, X., Ma, Y., Li, J., Xie, L., 2023. Simultaneous enhancement on lignocellulose degradation and humic acid formation using the electric field coupled with an iron anode in the co-composting of food waste and agricultural waste. Chem Eng J 475, 145846. https://doi.org/10.1016/j.cej.2023.145846.
[37] Santos-Pereira, C., Sousa, J., Costa, Â.M.A., Santos, A.O., Rito, T., Soares, P., Franco-Duarte, R., Silvério, S.C., Rodrigues, L.R., 2023. Functional and sequence-based metagenomics to uncover carbohydrate-degrading enzymes from composting samples. Appl Microbiol Biotechnol 107, 5379–5401. https://doi.org/10.1007/s00253-023-12627-9.
[38] Wang, S., Meng, Q., Zhu, Q., Niu, Q., Yan, H., Li, K., Li, G., Li, X., Liu, H., Liu, Y., Li, Q., 2021. Efficient decomposition of lignocellulose and improved composting performances driven by thermally activated persulfate based on metagenomics analysis. Sci Total Environ 794, 148530. https://doi.org/10.1016/j.scitotenv.2021.148530.
[39] Yin, Y., Yang, C., Tang, J., Gu, J., Li, H., Duan, M., Wang, X., Chen, R., 2021. Bamboo charcoal enhances cellulase and urease activities during chicken manure composting: roles of the bacterial community and metabolic functions. J Environ Sci 108, 84–95. https://doi.org/10.1016/j.jes.2021.02.007.
[40] Bohacz, J., Korniłłowicz-Kowalska, T., 2009. Changes in enzymatic activity in composts containing chicken feathers. Bioresour Technol 100, 3604–3612. https://doi.org/10.1016/j.biortech.2009.02.042.
[41] Huang, Y., Li, D., Wang, L., Yong, C., Sun, E., Jin, H., Huang, H., 2019. Decreased enzyme activities, ammonification rate, and ammonifiers contribute to higher nitrogen retention in hyperthermophilic pretreatment composting. Bioresour Technol 272, 521–528. https://doi.org/10.1016/j.biortech.2018.10.070.
[42] You, X., Wang, S., Chen, J., 2024. Magnetic biochar accelerates microbial succession and enhances assimilatory nitrate reduction during pig manure composting. Environ Int 184, 108469. https://doi.org/10.1016/j.envint.2024.108469.
[43] Li, S., Kang, J., Wu, Z., Sun, Y., Tu, X., Guo, Y., Mao, L., Yang, Y., Yao, W., Ge, J., 2025. Mechanisms of phosphorus conversion in chicken manure and straw composting systems regulated by flax-retting wastewater and a combination of flax-retting wastewater and biochar. Chem Eng J 507, 160773. https://doi.org/10.1016/j.cej.2025.160773.
[44] Zhou, Z., Liu, S., Saleem, M., Liu, F., Hu, R., Su, H., Dong, D., Luo, Z., Wu, Y., Zhang, Y., He, Z., Wang, C., 2025. Unraveling phase-dependent variations of viral community, virus-host linkage, and functional potential during manure composting process. Bioresour Technol 419, 132081. https://doi.org/10.1016/j.biortech.2025.132081.
[45] Kong, W., Sun, B., Zhang, J., Zhang, Y., Gu, L., Bao, L., Liu, S., 2020. Metagenomic analysis revealed the succession of microbiota and metabolic function in corncob composting for preparation of cultivation medium for Pleurotus ostreatus. Bioresour Technol 306, 123156. https://doi.org/10.1016/j.biortech.2020.123156.
[46] Wang, C., Wang, Y., Ru, H., He, T., Sun, N., 2021. Study on microbial community succession and functional analysis during biodegradation of mushroom residue. Biomed Res Int 2021, 6620574. https://doi.org/10.1155/2021/6620574.
[47] He, Y., Zhang, Y., Huang, X., Xu, J., Zhang, H., Dai, X., Xie, L., 2022. Deciphering the internal driving mechanism of microbial community for carbon conversion and nitrogen fixation during food waste composting with multifunctional microbial inoculation. Bioresour Technol 360, 127623. https://doi.org/10.1016/j.biortech.2022.127623.
[48] Che, J., Bai, Y., Li, X., Ye, J., Liao, H., Cui, P., Yu, Z., Zhou, S., 2021. Linking microbial community structure with molecular composition of dissolved organic matter during an industrial-scale composting. J Hazard Mater 405, 124281. https://doi.org/10.1016/j.jhazmat.2020.124281.
[49] Wang, G., Liu, H., Gong, P., Wang, J., Dai, X., Wang, P., 2022. Insight into the evolution of antibiotic resistance genes and microbial community during spiramycin fermentation residue composting process after thermally activated peroxydisulfate pretreatment. J Hazard Mater 424, 127287. https://doi.org/10.1016/j.jhazmat.2021.127287.
[50] De Corato, U., Patruno, L., Avella, N., Lacolla, G., Cucci, G., 2019. Composts from green sources show an increased suppressiveness to soilborne plant pathogenic fungi: Relationships between physicochemical properties, disease suppression, and the microbiome. Crop Prot 124, 104870. https://doi.org/10.1016/j.cropro.2019.104870.
[51] Matheri, F., Kambura, A.K., Mwangi, M., Karanja, E., Adamtey, N., Wanjau, K., Mwangi, E., Tanga, C.M., Bautze, D., Runo, S., 2023. Evolution of fungal and non-fungal eukaryotic communities in response to thermophilic co-composting of various nitrogen-rich green feedstocks. PLoS One 18, e0286320. https://doi.org/10.1371/journal.pone.0286320.
[52] Jaiswal, D., Pandey, J., 2018. Impact of heavy metal on activity of some microbial enzymes in the riverbed sediments: Ecotoxicological implications in the Ganga River (India). Ecotoxicol Environ Saf 150, 104–115. https://doi.org/10.1016/j.ecoenv.2017.12.015.
[53] Yang, B., Li, X., Lin, Z., Hu, D., Liu, Y., Pan, X., 2020. Evolution of enzyme activity, heavy metals bioavailability, and microbial community in different temperature stages of the co-bioevaporation process. Waste Manag 102, 751–762. https://doi.org/10.1016/j.wasman.2019.11.044.
[54] Cheng, Y., Wan, W., 2023. Strong linkage between nutrient-cycling functional gene diversity and ecosystem multifunctionality during winter composting with pig manure and fallen leaves. Sci Total Environ 867, 161529. https://doi.org/10.1016/j.scitotenv.2023.161529.
[55] Xue, K., Zhou, J., Van Nostrand, J., Mench, M., Bes, C., Giagnoni, L., Renella, G., 2018. Functional activity and functional gene diversity of a Cu-contaminated soil remediated by aided phytostabilization using compost, dolomitic limestone, and a mixed tree stand. Environ Pollut 242, 229–238. https://doi.org/10.1016/j.envpol.2018.06.057.
[56] Dang, Q., Wang, Y., Xiong, S., Yu, H., Zhao, X., Tan, W., Cui, D., Xi, B., 2021. Untangling the response of fungal community structure, composition, and function in soil aggregate fractions to food waste compost addition. Sci Total Environ 769, 145248. https://doi.org/10.1016/j.scitotenv.2021.145248.
[57] Wang, G., Kong, Y., Yang, Y., Ma, R., Shen, Y., Li, G., Yuan, J., 2022. Superphosphate, biochar, and a microbial inoculum regulate phytotoxicity and humification during chicken manure composting. Sci Total Environ 824, 153958. https://doi.org/10.1016/j.scitotenv.2022.153958.
[58] Wang, C., Dong, D., Wang, H., Müller, K., Qin, Y., Wang, H., Wu, W., 2016. Metagenomic analysis of microbial consortia enriched from compost: new insights into the role of Actinobacteria in lignocellulose decomposition. Biotechnol Biofuels 9, 22. https://doi.org/10.1186/s13068-016-0440-2.
[59] Chen, W., Xu, J., Wang, S., Chen, Z., Dong, S., 2025. Key drivers of heavy metal bioavailability in river sediments and microbial community responses under long-term high-concentration pollution. Environ Res 265, 120375. https://doi.org/10.1016/j.envres.2024.120375.